# Stability Theory of the Magnetic Phases for a Simple Model of the Transition Metals*†

DAVID R. PENN‡
*Department of Physics and Institute for the Study of Metals, University of Chicago, Chicago, Illinois*

(Received 4 August 1965)

A semiquantitative explanation of the observed distribution of magnetism in the transition metals and alloys is made based on a highly simplified quasiparticle band model. It depends on only two parameters, the valence (number of $d$ electrons) of the metal and the ratio of quasiparticle interaction strength to bandwidth, $C_0/E''$. The quantity $C_0/E''$ increases with valence and also increases as one goes from the $5d$ transition metals to the $3d$ transition metals. Ferromagnetism is found to be most likely for those metals with large $C_0/E''$ and a valence well away from five. Antiferromagnetism is found to occur for a valence of around five, as do the more complex states such as the ferrimagnetic and spiral-spin-density-wave states, which are explicitly described. It is suggested that the peak in the specific heat of the transition-metal alloys that occurs as one alloys across the $3d$ transition series is closely related to changes in the band structure caused by ordering, at least for the Cr-Mn system.

## I. INTRODUCTION

IT has been known for some time that the $d$ electrons in the transition metals should be treated as itinerant rather than localized electrons. This is most clearly evidenced by the large linear specific heats, the nonintegral magnetic moments in the magnetic metals, and the fact that band calculations indicate the $d$ bandwidth to be substantial. More recently, Fermi surface studies have given still more direct and unequivocal support to the itinerant model. Itinerant electron models have been proposed to explain the ferromagnetism found in the transition metals, e.g., those put forward by Bloch,[1] Slater,[2] Van Vleck[3] (not purely itinerant), Mott and Stevens,[4] Kanamori,[5] and Herring.[6] Similarly, it has been possible to treat the phenomenon of antiferromagnetism within the itinerant electron model, and work in this field has been done by Slater,[7] des Cloizeaux,[8] Overhauser,[9] Tachiki and Nagamiya,[10] and others. Up to this point no band treatment of ferrimagnetism has been developed despite the fact that it has been observed in $CrPt_3$ and in more complicated alloys such as $Mn_2Sb$, $Mn_3As$, and others. Furthermore, an ordered ferromagnetic alloy will have a spatial distribution of magnetic moments such that it should be considered as ferrimagnetic.

The observed distribution of magnetism in the transition metals is remarkably simple. With reference to the part of the periodic table that comprises the transition elements, one finds ferromagnetism in the upper right-hand corner and more complex magnetic behavior in the upper center of the table. The purpose of this paper is to study the incidence and distribution of magnetism in the transition metals and their alloys on the basis of a simple model that is capable of describing ferromagnetic, antiferromagnetic, ferrimagnetic and even more complex states. Simple as the model is, the particular numerical values of the parameters of the model can still be put into a rough correspondence with position in the periodic table.

In Sec. II we describe the simple model. In Sec. III we introduce the concept of a phase diagram defined relative to the parameters of the model. We use the phase diagram to indicate the relative stability of various magnetic phases and so correlate the copious numerical results obtained from the model. The methods used to construct the phase diagram are discussed; they involve calculation of appropriate response functions and an actual calculation of the energies of various magnetic states. The correspondence of the model to actual transition metals and alloys is discussed semiquantitatively. In Sec. IV it is shown how various types of magnetic states may be constructed and their energies calculated within the framework of the model. Of these, the paramagnetic, ferromagnetic, antiferromagnetic, ferrimagnetic, and spiral-spin-density-wave states are chosen for explicit study. In Sec. V the method used in constructing the response functions is discussed. In Secs. VI through X those states described above are studied individually and a number of phase diagrams are constructed. In Sec. XI the question of local moment formation is studied within the context of our model using the theory developed by Wolff[11] and numerical results are presented.

## II. MODEL

We shall now describe the model used to treat the transition metals and alloys. The electrons are divided into two classes, $s$ like and $d$ like. The magnetic polarization of the $s$ like electrons is induced by that of the $d$

* Work supported in part by the National Science Foundation and the U. S. Office of Naval Research.

† Submitted in partial fulfillment of the requirements for the degree of Doctor of Philosophy at the University of Chicago.

‡ Xerox predoctoral fellow.

[1] F. Bloch, Z. Physik **57**, 545 (1929).
[2] J. C. Slater, Phys. Rev. **49**, 537 (1936).
[3] J. H. Van Vleck, Rev. Mod. Phys. **25**, 220 (1953).
[4] N. F. Mott and K. W. H. Stevens, Phil. Mag. **2**, 1364 (1957).
[5] J. Kanamori, Progr. Theoret. Phys. (Kyoto) **30**, 275 (1963).
[6] C. Herring (to be published).
[7] J. C. Slater, Phys. Rev. **82**, 538 (1951).
[8] J. des Cloizeaux, J. Phys. Radium **20**, 606, 751 (1959).
[9] A. W. Overhauser, Phys. Rev. **128**, 1437 (1962).
[10] M. Tachiki and T. Nagamiya, Phys. Letters **3**, 214 (1962).
[11] P. A. Wolff, Phys. Rev. **124**, 1030 (1961).

electrons and can, in principle, be treated by perturbation theory, thus our primary concern shall be with the $d$ electrons which are treated within a simplified version of the Landau quasiparticle picture at zero temperature.

In the paramagnetic state, the quasiparticles occupy a single band appropriate to the tight-binding approximation for a crystal of cubic symmetry. The atomic wave functions used in the tight binding scheme are assumed to have $s$ like symmetry and next-nearest-neighbor overlap is neglected. We shall indicate which results depend essentially on this choice of band structure and attempt, as well, to point out permissible generalizations. Within the approximations described above, the band part of the energy appropriate to a particle of wave number $\mathbf{k}$ is

$$\epsilon_{\mathbf{k}}=-E''(\cos k_x a+\cos k_y a+\cos k_z a), \qquad (2.1)$$

where $a$ is the nearest-neighbor distance in the crystal and the components of $\mathbf{k}$ satisfy

$$-\pi/a<k_j<\pi/a; \quad j=x, y, z. \qquad (2.2)$$

The function $\epsilon_{\mathbf{k}}$ is plotted in Fig. 1 for $\mathbf{k}$ in the [111] direction. The density of states corresponding to $\epsilon_{\mathbf{k}}$ is also shown in Fig. 1 and is in only very rough agreement with the actual density of states found in the transitions metals; the present curve falls off too slowly at the ends and the shape is otherwise too simple.

The particle-particle interaction is treated in the self-consistent-field (SCF) approximation and consequently is described by

$$H_{\text{int}}=C_0[\textstyle\sum_{l\sigma}(\langle c_{l\sigma}^{\dagger}c_{l\sigma}\rangle c_{l\bar{\sigma}}^{\dagger}c_{l\bar{\sigma}}-\langle c_{l\sigma}^{\dagger}c_{l\bar{\sigma}}\rangle c_{l\bar{\sigma}}^{\dagger}c_{l\sigma}] \qquad (2.3)$$

in second quantization. Here $c_{l\sigma}^{\dagger}(c_{l\sigma})$ represents the creation (destruction) operators of an electron in a Wannier state of spin $\sigma$ on site $l$; $C_0$ is to be interpreted as the interaction strength between quasiparticles. The quasiparticle screening serves to eliminate interactions between particles on different sites. The total energy of the system is given by

$$E_{\text{tot}}=\textstyle\sum_{\mathbf{k}\sigma}\epsilon_{\mathbf{k}}\langle a_{\mathbf{k}\sigma}^{\dagger}a_{\mathbf{k}\sigma}\rangle+\frac{1}{2}C_0\sum_{l\sigma}(\langle c_{l\sigma}^{\dagger}c_{l\sigma}\rangle\langle c_{l\sigma}^{\dagger}c_{l\bar{\sigma}}\rangle - \langle c_{l\sigma}^{\dagger}c_{l\bar{\sigma}}\rangle\langle c_{l\bar{\sigma}}^{\dagger}c_{l\sigma}\rangle), \qquad (2.4)$$

where

$$a_{\mathbf{k}\sigma}=(1/\sqrt{N})\textstyle\sum_l \exp(-i\mathbf{k}\cdot\mathbf{R}_l)c_{l\sigma} \qquad (2.5)$$

(and similarly $a_{\mathbf{k}\sigma}^{\dagger}$) is the destruction (creation) operator of an electron in a Bloch state $\mathbf{k}\sigma$; $N$ is the number of unit cells in the crystal. We shall see shortly that in the case of a ferromagnetic state the model reduces to the usual Slater[2] band theory of ferromagnetism in which the spin-up and spin-down electron bands are identical in shape but separated from each other by an energy difference referred to as the exchange splitting, and the total energy of the system contains a term proportional to the square of the magnetization.

Within the model which we have described, the Hamiltonian is specified by only two parameters; the total number of particles $n$ and the strength of the electron interaction $C_0$ measured relative to $E''$. An insulator may be described by only one parameter, $C_0/E''$, since the band is totally filled; this represents a crucial difference between the two states. The parameters $C_0$ and $E''$ being quasiparticle parameters should, in fact, depend on the state of magnetization of the system but we shall neglect this effect and take them to be the same for all states. Within the quasiparticle model we shall investigate the energetic stability of one state with respect to another, but it should be borne in mind that the model is not strictly valid for calculating the actual cohesive energy of a state.

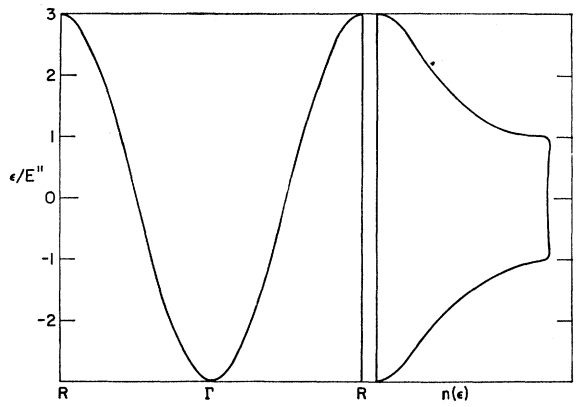


FIG. 1. The energy band $\epsilon_{\mathbf{k}}=\cos k_x a+\cos k_y a+\cos k_z a$ in the [111] direction and the density of states corresponding to $\epsilon_{\mathbf{k}}$.

## III. PHASE DIAGRAM

For a given $C_0/E''$ and $n$ there may be more than one type of state which are self-consistent eigenstates of our Hamiltonian. We are specifically interested in the state of lowest energy for each $C_0/E''$ and $n$. For different values of $C_0/E''$ and $n$, states of different character may correspond to states of lowest energy. Thus, we can construct a phase diagram in which the total number of particles $n$ is given by the abscissas, and the relative interaction strength $C_0/E''$ is given by the ordinates; different regions in this phase diagram will correspond to stability of different phases. The problem we set for ourselves in the present paper is to establish by direct quantitative calculation at least some of the phase boundaries in this phase diagram.

There are two methods at our disposal for constructing the phase diagram: (1) we can compare the total energies of each of the various states that exist at a given point of the phase diagram, or (2) we can assume that a state is stable at some point of phase space and then test this assumption by computing the response function of the state to a time-independent, spin-dependent external potential. A negative value of the response function would indicate thermodynamic instability with respect to a spontaneous spin distribution corresponding to that induced by the external field. This response function method is by far the easier of the two employed

here: it requires only a knowledge of the wave function of the state whose stability we are examining; it does not require a detailed knowledge of the other states that may exist at the same phase point. Unfortunately this method has a disadvantage which stems from the fact that the response function is calculated by means of perturbation theory or its equivalent. The method tests only for stability against an infinitesimal external perturbation which can be misleading in the case of a first-order phase transition where the phase transition occurs while the state is still stable against infinitesimal perturbations.

Having constructed a phase diagram, it is necessary to establish, at least roughly, the manner in which a given transition metal or alloy corresponds to a given point on the diagram. The correspondence between the average valence of the metal or alloy and the number of electrons in the model is immediate, apart from the uncertainty with respect to $s$ electrons. In addition, it is possible to establish a qualitative correspondence between position in the periodic table and $C_0/E''$. One would expect that for a given row of the periodic table, $C_0$ will increase as the $d$ shell is filled since the electrons become more tightly bound as the nuclear charge increases. A Hartree-Fock calculation by Watson[12] for the $3d$ transition atoms indicates that the Slater $F$ Coulomb integrals increase by approximately 50% as one goes from Ti to Ni. The bandwidths of the $3d$ transition metals have been calculated by Mattheiss[13] who finds that they decrease by more than a factor of 2 on going from Ti to Ni so that we may expect $C_0/E''$ to increase by a factor of about 3 as one moves from Ti to Ni. A similar variation in $C_0/E''$ is to be expected in going from Zr to Pd and from Hf to Pt. Also, for a given valence, we may expect a large increase in $C_0/E''$ as we move from the $5d$ transition series to the $3d$ series because of the decrease in the radius of the $d$ electrons.

## IV. CONSTRUCTION AND SELECTION OF STATES

The states whose properties we wish to examine in detail will now be discussed. The simplest of these are the paramagnetic and ferromagnetic states. Furthermore, various authors have pointed out the feasibility of describing the antiferromagnetic state within the Bloch itinerant-electron framework. The antiferromagnetic state is characterized by a spatially changing component of magnetization which varies in such a way that the net magnetization of the system is zero. We shall show explicitly that this state and more complicated states (e.g., ferrimagnetic) can be made eigenfunctions of the SCF equations.

Let us assume that the SCF Hamiltonian is diagonalized by the transformation

$$\beta_{\mathbf{k}}=A_{\mathbf{k}}a_{\mathbf{k}\uparrow}+B_{\mathbf{k}}a_{\mathbf{k}\downarrow}+C_{\mathbf{k}}a_{\mathbf{k}+\mathbf{q}\uparrow}+D_{\mathbf{k}}a_{\mathbf{k}+\mathbf{q}\downarrow}, \tag{4.1}$$

where $a_{\mathbf{k}\sigma}$ is defined in (2.5). Because of higher order Bragg reflections, the Hamiltonian will not be expressible as a sum of number operators $\beta_{\mathbf{k}}^{\dagger}\beta_{\mathbf{k}}$ unless terms of the form $a_{\mathbf{k}+n\mathbf{q}\sigma}$ are added to $\beta_{\mathbf{k}}$. Thus, while one may readily investigate the stability of a uniform (i.e., paramagnetic or ferromagnetic) state, the actual self-consistent construction of the energy and wave function of a stable state of arbitrary $\mathbf{q}$ is prohibitively difficult. To avoid this difficulty in the explicit construction of states we may restrict ourselves to the case $\mathbf{q}=\mathbf{Q}$ where

$$\mathbf{Q}=\mathbf{G}/2 \tag{4.2}$$

and $\mathbf{G}$ is a reciprocal lattice vector. Thus, the operator transformation is given by

$$\gamma_{\mathbf{k}}=B_1a_{\mathbf{k}\uparrow}+B_2a_{\mathbf{k}\downarrow}+B_3a_{\mathbf{k}+\mathbf{Q}\uparrow}+B_4a_{\mathbf{k}+\mathbf{Q}\downarrow}, \tag{4.3}$$

since $\mathbf{k}+2\mathbf{Q}=\mathbf{k}$ in the reduced zone.

The various thermodynamic averages that result from the self-consistent part of the Hamiltonian are denoted by

$$A_{0\uparrow\downarrow}=-C_0\textstyle\sum_{\mathbf{k}}\langle a_{\mathbf{k}\downarrow}^{\dagger}a_{\mathbf{k}\uparrow}\rangle, \tag{4.4a}$$

$$A_{0\uparrow}=C_0\textstyle\sum_{\mathbf{k}}\langle a_{\mathbf{k}\downarrow}^{\dagger}a_{\mathbf{k}\downarrow}\rangle, \tag{4.4b}$$

$$A_{0\downarrow}=C_0\textstyle\sum_{\mathbf{k}}\langle a_{\mathbf{k}\uparrow}^{\dagger}a_{\mathbf{k}\uparrow}\rangle, \tag{4.4c}$$

$$A_{Q\uparrow\downarrow}=-C_0\textstyle\sum_{\mathbf{k}}\langle a_{\mathbf{k}+\mathbf{Q}\downarrow}^{\dagger}a_{\mathbf{k}\uparrow}\rangle, \tag{4.4d}$$

$$A_{Q\uparrow}=C_0\textstyle\sum_{\mathbf{k}}\langle a_{\mathbf{k}+\mathbf{Q}\downarrow}^{\dagger}a_{\mathbf{k}\downarrow}\rangle, \tag{4.4e}$$

$$A_{Q\downarrow}=C_0\textstyle\sum_{\mathbf{k}}\langle a_{\mathbf{k}+\mathbf{Q}\uparrow}^{\dagger}a_{\mathbf{k}\uparrow}\rangle. \tag{4.4f}$$

The use of Eqs. (4.3) in (4.4) yields

$$A_{0\uparrow\downarrow}=-(C_0/N)\textstyle\sum_{\mathbf{k}}F_{\mathbf{k}}(B_1B_2+B_3B_4), \tag{4.5a}$$

$$A_{0\uparrow}=(C_0/N)\textstyle\sum_{\mathbf{k}}F_{\mathbf{k}}(B_2^2+B_4^2), \tag{4.5b}$$

$$A_{0\downarrow}=(C_0/N)\textstyle\sum_{\mathbf{k}}F_{\mathbf{k}}(B_1^2+B_3^2), \tag{4.5c}$$

$$A_{Q\uparrow\downarrow}=-(C_0/N)\textstyle\sum_{\mathbf{k}}F_{\mathbf{k}}(B_1B_4+B_2B_3), \tag{4.5d}$$

$$A_{Q\uparrow}=2(C_0/N)\textstyle\sum_{\mathbf{k}}F_{\mathbf{k}}B_2B_4, \tag{4.5e}$$

$$A_{Q\downarrow}=2(C_0/N)\textstyle\sum_{\mathbf{k}}F_{\mathbf{k}}B_1B_3, \tag{4.5f}$$

where $F_{\mathbf{k}}$ is the occupation number of the state defined by $\gamma_{\mathbf{k}}$. The single-particle energy $E_{\mathbf{k}}$ corresponding to the transformation $\gamma_{\mathbf{k}}$ is found from the condition $[\gamma_{\mathbf{k}}^{\dagger},H]=E_{\mathbf{k}}\gamma_{\mathbf{k}}^{\dagger}$ which is equivalent to diagonalizing the matrix

$$\|E\|=\begin{vmatrix} \epsilon_{\mathbf{k}}+A_{0\uparrow}-E_{\mathbf{k}} & A_{0\uparrow\downarrow} & A_{Q\uparrow} & A_{Q\uparrow\downarrow} \\ A_{0\uparrow\downarrow} & \epsilon_{\mathbf{k}}+A_{0\downarrow}-E_{\mathbf{k}} & A_{Q\uparrow\downarrow} & A_{Q\downarrow} \\ A_{Q\uparrow} & A_{Q\uparrow\downarrow} & \epsilon_{\mathbf{k}+\mathbf{Q}}+A_{0\uparrow}-E_{\mathbf{k}} & A_{0\uparrow\downarrow} \\ A_{Q\uparrow\downarrow} & A_{Q\downarrow} & A_{0\uparrow\downarrow} & \epsilon_{\mathbf{k}+\mathbf{Q}}+A_{0\downarrow}-E_{\mathbf{k}} \end{vmatrix}. \tag{4.6}$$

[12] R. E. Watson, Phys. Rev. 119, 1934 (1960).
[13] L. F. Mattheiss, Phys. Rev. 134, A970 (1964).

Diagonalization of $\mathbf{E}$ will give both $E_k$ and the $B_i$ in terms of the matrix elements $A_0$, $A_Q$ of Eq. (4.5). Hence, Eqs. (4.5) represent a set of simultaneous equations (self-consistency equations) for the matrix elements $A$.

The magnetization and the number of particles of a state are given by

$$\mathbf{M}(\mathbf{q})=(1/N)\sum_l \exp(i\mathbf{q}\cdot\mathbf{R}_l)\mathbf{M}_l \tag{4.7a}$$

$$n(\mathbf{q})=(1/N)\sum_l \exp(i\mathbf{q}\cdot\mathbf{R}_l)n_l \tag{4.7b}$$

as functions of wave number $\mathbf{q}$, where

$$\mathbf{M}_l=\mu_B\sum_{\sigma\sigma'}\langle l\sigma|\hat{x}\sigma_x+\hat{y}\sigma_y+\hat{z}\sigma_z|l\sigma'\rangle\langle c_{l\sigma}{}^\dagger c_{l\sigma'}\rangle, \tag{4.8a}$$

$$n_l=\sum_\sigma\langle c_{l\sigma}{}^\dagger c_{l\sigma}\rangle, \tag{4.8b}$$

and $|l\sigma\rangle$ denotes a Wannier function. On using Eqs. (4.3) and (4.5) in conjunction with Eq. (4.7) one obtains

$$M_x(0)=-(2\mu_B/C_0)A_{0\uparrow\downarrow}, \tag{4.9a}$$

$$M_x(\mathbf{Q})=-(2\mu_B/C_0)A_{Q\uparrow\downarrow}, \tag{4.9b}$$

$$M_z(0)=(\mu_B/C_0)(A_{0\downarrow}-A_{0\uparrow}), \tag{4.9c}$$

$$M_z(\mathbf{Q})=(\mu_B/C_0)(A_{Q\uparrow}-A_{Q\downarrow}) \tag{4.9d}$$

$$n(0)=n, \tag{4.9e}$$

$$n(\mathbf{Q})=(1/C_0)(A_{Q\uparrow}+A_{Q\downarrow}). \tag{4.9f}$$

The quantity $M_y$ is found to be zero due to the fact that we may choose the $B_i$ to be real for the special values $\mathbf{Q}$ of $\mathbf{q}$ used here. The nonzero value of $n(\mathbf{Q})$ implies a nonuniform charge distribution which should, in fact, be screened. However, in the interests of making actual numerical calculations, we shall not complicate the theory further but shall bear in mind that such screening would reduce the energy of a state with nonzero $n(\mathbf{Q})$.

The total energy is found from Eq. (2.4) to be given by

$$E_{\text{tot}}=\sum_k F_k E_k-(A_{0\uparrow}A_{0\downarrow}+A_{Q\uparrow}A_{Q\downarrow}-A_{0\uparrow\downarrow}{}^2-A_{Q\uparrow\downarrow}{}^2)(N/C_0). \tag{4.10}$$

The concern will now be with a limited number of the infinitely many possible SCF eigenstates. We shall only consider states whose properties show no spatial variation (paramagnetic and ferromagnetic states) or states which have properties that exhibit spatial variation characterized by $\mathbf{Q}$ (e.g., the antiferromagnetic state). We limit ourselves to the case $\mathbf{Q}=\pi/a(1,1,1)$; thus $e^{i\mathbf{Q}\cdot\mathbf{r}}$ changes sign as we move from one lattice site to the next with the result that the crystal symmetry is transformed from simple cubic to face-centered cubic. We shall further limit our study to the following states with their corresponding nonzero $A$'s:

paramagnetic: $A_{0\uparrow}=A_{0\downarrow}$, (4.11a)

ferromagnetic: $A_{0\uparrow}, A_{0\downarrow}$, (4.11b)

antiferromagnetic: $A_{0\uparrow}=A_{0\downarrow}, A_{Q\uparrow\downarrow}$, (4.11c)

or

$A_{0\uparrow}=A_{0\downarrow}, A_{Q\uparrow}=A_{Q\downarrow}$, (4.11d)

spiral-spin-density wave (SSDW): $A_{0\uparrow}, A_{0\downarrow}, A_{Q\uparrow\downarrow}$, (4.11e)

ferrimagnetic: $A_{0\uparrow}, A_{0\downarrow}, A_{Q\uparrow}, A_{Q\downarrow}$. (4.11f)

TABLE I. The magnetization and number of particles of the states listed in Eqs. (4.11).

| | Para | Ferro | Anti 1[a] | Anti 2[a] | Ferri | SSDW |
|---|---|---|---|---|---|---|
| $M_z(0)$ | 0 | $A1$ | 0 | 0 | $A1$ | $A1$ |
| $M_z(Q)$ | 0 | 0 | 0 | $A2$ | $A2$ | 0 |
| $M_x(Q)$ | 0 | 0 | $A3$ | 0 | 0 | $A3$ |
| $n(0)$ | $A4$ | $A4$ | $A4$ | $A4$ | $A4$ | $A4$ |
| $n(Q)$ | 0 | 0 | 0 | 0 | $A5$ | 0 |

$A1=[A_\downarrow(0)-A_\uparrow(0)]/C_0$ $\quad A2=[A_\downarrow(Q)-A_\uparrow(Q)]/C_0$
$A3=-2A_{\uparrow\downarrow}(Q)/C_0$ $\quad A4=n/N$ $\quad A5=[A_\downarrow(Q)+A_\uparrow(Q)]/C_0$

[a] The states Anti 1 and Anti 2 differ only in the direction of quantization.

Table I gives the magnetization and the number of particles of these states. The two antiferromagnetic states differ only in the choice of the axis of spin quantization. In Table II we have indicated which states may transform into one another by means of a second-order phase transition along some boundary line of the phase diagram. The remaining transitions will be first order.

We discuss in detail in Secs. VI to X each of the states under consideration after presenting in Sec. V the necessary preliminary material on response functions $\chi(\mathbf{q})$. Although we have restricted ourselves to the explicit construction of states containing only $\mathbf{Q}=\pi/a(1,1,1)$ it will be feasible to construct $\chi(\mathbf{q})$ for arbitrary wave number for at least the paramagnetic and ferromagnetic states. The greater ease of the response function method for testing the relative stability of different phases thus permits us to test the stability of the paramagnetic state against general antiferromagnetic states. We may thus check, within the limitations of our model, the currently common ideas about the close relationship between spin wave number and special features of the Fermi surface.

## V. RESPONSE FUNCTIONS

We shall now concern ourselves with calculating the linear response of a state to an external potential. The application of an external magnetic field having a poten-

TABLE II. States which may transform into one another through a second-order phase transformation along a line in phase space are indicated by $X$'s. The remaining transformations will be first order or absent and are indicated by zeros. The states are those listed in Eq. (4.11).

| | Para | Ferro | Anti 1[a] | Anti 2[a] | Ferri | SSDW |
|---|---|---|---|---|---|---|
| Para | | | | | | |
| Ferro | $X$ | | | | | |
| Anti 1 | $X$ | 0 | | | | |
| Anti 2 | $X$ | $X$ | 0 | | | |
| Ferri | 0 | $X$ | 0 | $X$ | | |
| SSDW | 0 | $X$ | $X$ | 0 | 0 | |

[a] The states Anti 1 and Anti 2 differ only in the direction of quantization.

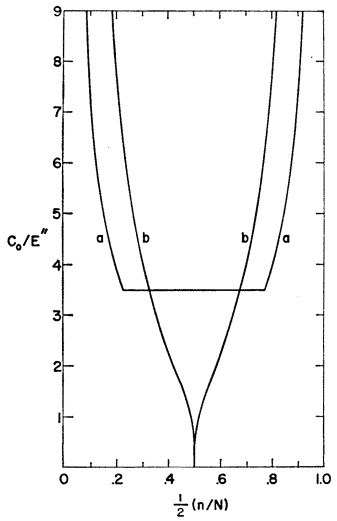


FIG. 2. The phase boundaries determined by an infinite value of the paramagnetic susceptibility for the cases $\mathbf{q}=0$ (line *a*) and $\mathbf{q}=\mathbf{Q}$ (line *b*).

tial $H'$ will cause a change $H_1$ in the SCF Hamiltonian

$$H_1=H'+V_R, \tag{5.1}$$

where $V_R$ is due to the induced change in the particle distribution. A corresponding change $\rho_1$ is induced in the one-particle density matrix (it is convenient to use first quantization in this section). The response $V_R$ is related to $\rho_1$ by[14]

$$\langle l\sigma|V_R|l\sigma\rangle=\sum_{msns'}\langle ms|\rho_1|ns'\rangle\langle ns',l\sigma|O|l'\sigma',ms\rangle, \tag{5.2}$$

where $|l'\sigma'\rangle$ denotes a Wannier function of spin $\sigma'$ located at site $l'$ and $O$ the operator representing the quasiparticle interaction. From Eq. (2.3) we have

$$\langle ns',l\sigma|O|l'\sigma',ms\rangle=C_0\delta_{n,l,l',m}(\delta_{s,s'}\delta_{\sigma,\sigma'}-\delta_{s',\sigma'}\delta_{s,\sigma}). \tag{5.3}$$

Equation (5.2) becomes

$$\langle l\sigma|V_R|l'\sigma'\rangle=C_0\delta_{l,l'}(\delta_{\sigma,\sigma'}\langle l\bar{\sigma}|\rho_1|l\bar{\sigma}\rangle -\delta_{\sigma,\bar{\sigma}'}\langle l\sigma|\rho_1|l\bar{\sigma}\rangle), \tag{5.4}$$

where $\bar{\sigma}$ represents the opposite spin state of $\sigma$.

It is shown in the Appendix that the matrix element of $\rho_1$ taken with respect to wave functions which diagonalize the unperturbed Hamiltonian $H_0$ is given by

$$\langle u|\rho_1|v\rangle=\langle u|H_1|v\rangle \times(F(\epsilon_u)-F(\epsilon_v))/(\epsilon_u-\epsilon_v);\quad u\neq v \tag{5.5a}$$

$$\langle u|\rho_1|u\rangle=(\langle u|H_1|u\rangle-\mu_1)(\partial F/\partial\epsilon)_u, \tag{5.5b}$$

where $\epsilon_u$ is an eigenvalue of $H_0$,

$$F(\epsilon_u)=\{1+\exp[\beta(\epsilon_u-\mu_0)]\}^{-1},$$

$\mu_0$ is the unperturbed Fermi energy, and $\mu_1$ is the change in Fermi energy induced by $H'$. The quantity $\mu_1$ is determined from the condition $\mathrm{Tr}\rho_1=0$ to be

$$\mu_1=\sum_u\langle u|H_1|u\rangle\left(\frac{\partial F}{\partial\epsilon}\right)_u\Big/\sum_u\left(\frac{\partial F}{\partial\epsilon}\right)_u. \tag{5.6}$$

We see from Eqs. (5.4), (5.5), and (5.6) that $V_R$ is linearly related to $H'$.

The change in the magnetization at site $l$ due to $H$ is given by

$$\delta\mathbf{M}_l=\mu_B\sum_\sigma\langle l\sigma|\boldsymbol{\sigma}\rho_1|l\sigma\rangle. \tag{5.7}$$

We find

$$\delta M_{zl}=(\mu_B/C_0) \times(\langle l\downarrow|V_R|l\downarrow\rangle-\langle l\uparrow|V_R|l\uparrow\rangle), \tag{5.8a}$$

$$\delta M_{xl}+i\delta M_{yl}=-2(\mu_B/C_0)\langle l\downarrow|V_R|l\uparrow\rangle, \tag{5.8b}$$

$$\delta M_{xl}-i\delta M_{yl}=-2(\mu_B/C_0)\langle l\uparrow|V_R|l\downarrow\rangle. \tag{5.8c}$$

If $V_R$ is known [from Eqs. (5.4) and (5.5)] in terms of $H'$, we immediately can determine the change in magnetization $\delta\mathbf{M}_l$. The response functions $\chi_i$ are now defined by

$$\chi_i(\mathbf{q})=\delta M_i(\mathbf{q})/H_i'(\mathbf{q})\quad i=x,y,z, \tag{5.9}$$

where $H_i'(\mathbf{q})$ is the $\mathbf{q}$th Fourier transform of $H_i'(\mathbf{r})$. Thus $\chi_i(\mathbf{q})$ is evaluated by relating $\delta\mathbf{M}_i$ to $H_i'$.

## VI. PARAMAGNETIC STATE

The operator transformation [Eq. (4.3)] reduces to the identity transformation

$$\gamma_{k\uparrow}=a_{k\uparrow}, \tag{6.1a}$$

$$\gamma_{k\downarrow}=a_{k\downarrow}, \tag{6.1b}$$

for the paramagnetic state. The one-particle energies are (Fig. 1)

$$\epsilon_{k\sigma}=\epsilon_k+A_0, \tag{6.2}$$

where

$$A_0=\tfrac{1}{2}C_0n/N; \tag{6.3}$$

the total energy is

$$E=\sum_{k\sigma}F_{k\sigma}\epsilon_k+A_0^2N/C_0, \tag{6.4}$$

and, of course, we have

$$F_{k\uparrow}=F_{k\downarrow}. \tag{6.5}$$

To test the stability of the paramagnetic state against transformation to the antiferromagnetic phase we need only examine the sign of the $z$ component of the paramagnetic susceptibility $\chi_z(\mathbf{q})$ for all $\mathbf{q}$. The other components of $\chi$, because of the rotational invariance of the paramagnetic state, give nothing new. The susceptibility $\chi_z(\mathbf{q})$ is found from (A15) to be given by

$$\chi_z(\mathbf{q})=-2\mu_B^2\Gamma(\mathbf{q})/(1+C_0\Gamma(\mathbf{q})), \tag{6.6}$$

where

$$\Gamma(\mathbf{q})=(1/N)\sum_k(F_{k+q}-F_k)/(\epsilon_{k+q}-\epsilon_k). \tag{6.7}$$

The susceptibility $\chi_z(\mathbf{q}=0)$ is from (A16)

$$\chi_z(0)=2\mu_B^2\eta_0/(1-C_0\eta_0), \tag{6.8}$$

[14] M. H. Cohen, Phys. Rev. **130**, 1301 (1963).

where $\eta_0$ is the density of states at the Fermi energy of electrons of either spin. The $\mathbf{q}=0$ susceptibility changes sign at the line in phase space determined by

$$1=C_0\eta_0, \tag{6.9}$$

which is shown in Fig. 2 as line $a$ and is the standard condition for ferromagnetism (see for example Friedel *et al.*[15]). Below the line we have $\chi_z(0)>0$ so that the paramagnetic state is stable with respect to the ferromagnetic state, whereas above the line $\chi_z(0)<0$ and the ferromagnetic state has lower energy.

In the particular case of $\mathbf{Q}=\pi/a(1,1,1)$, we have

$$\epsilon_{\mathbf{k}+\mathbf{Q}}=-\epsilon_{\mathbf{k}}, \tag{6.10}$$

from which it follows that

$$\Gamma(\mathbf{Q})=\int_{-3E''}^{\epsilon_F}\frac{\eta_0(\epsilon)}{\epsilon}d\epsilon, \tag{6.11}$$

where $\epsilon_F$ is the Fermi energy of the paramagnetic state as measured from the center of the band. The line in phase space determined by

$$1+C_0\Gamma(\mathbf{Q})=0 \tag{6.12}$$

is shown in Fig. 2 as line $b$. Above the line $b$, $\chi_z(\mathbf{Q})$ is negative, meaning that the antiferromagnetic state with $\mathbf{Q}=\pi/a(1,1,1)$ has a lower energy than the paramagnetic state in that region.

The value of $C_0$ at which the paramagnetic state becomes unstable for a given $n$ is

$$(C_0)_{\text{crit}}=-1/\Gamma(\mathbf{q}_c), \tag{6.13}$$

where $\mathbf{q}_c$ is the value of $\mathbf{q}$ for which $\Gamma(\mathbf{q})$ is maximum. We note that $(C_0)_{\text{crit}}\to 0$ as $\epsilon_F\to 0$, i.e., in the middle of the band $\Gamma(\mathbf{Q})\to-\infty$. This is a specific feature of the band structure. In the case of a more general band structure, the smallest value of $(C_0)_{\text{crit}}$ will occur for the valence at which the Fermi surface most nearly coincides with a magnetic zone boundary (in our case the $\mathbf{q}=\mathbf{Q}$ zone boundary is determined by the condition $\epsilon_{\mathbf{k}}=\epsilon_{\mathbf{k}+\mathbf{Q}}$). As Overhauser has repeatedly emphasized, one may expect a continuous variation of the $\mathbf{q}$ for which antiferromagnetism occurs. In general, this $\mathbf{q}$ will be such as to maintain a maximum coincidence between the magnetic zone boundary and the Fermi surface. To explore this important point we can study $\chi(\mathbf{q})$ for more general $\mathbf{q}$'s. Clearly, for given valence, the paramagnetic state becomes unstable, for smallest $C_0$, for that $\mathbf{q}$ for which $\Gamma(\mathbf{q})$ is maximal. Because we are dealing with a very simple band structure, $\Gamma(\mathbf{q})$ varies smoothly with $\mathbf{q}$. Phillips[16] has argued on topological grounds that under such circumstances it is often sufficient to search only along symmetry lines for critical points in such functions, which is all we shall do here.

[15] J. Friedel, G. Leman, and S. Olszewski, J. Appl. Phys. **32**, 325S (1961).

[16] J. C. Phillips, Phys. Rev. **104**, 1263 (1956).

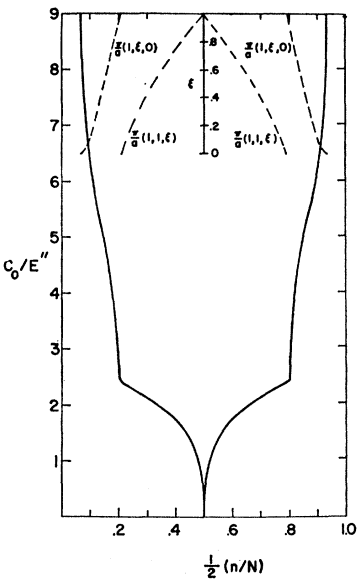


FIG. 3. The phase boundary above which the paramagnetic state is unstable. For $n/N>0.14$ the quantity $\mathbf{q}_c$ of Eq. (6.13) may be obtained from the upper portion of the figure; $\mathbf{q}_c=0$ for $n/N<0.14$.

The search for $\mathbf{q}_c$ can be carried out by numerical evaluation of $\Gamma(\mathbf{q})$. The lower curve of Fig. 3 shows the line determined by $\chi(\mathbf{q}_c)^{-1}=0$. The value of $\mathbf{q}_c$ corresponding to a point on that line may be found from the upper portion of the figure. From Eq. (6.7) one might expect that the largest contribution to $\Gamma(\mathbf{q}_c)$ will come from those points in momentum space for which $\mathbf{k}$ lies just inside the Fermi sphere and $\mathbf{k}+\mathbf{q}_c$ lies just outside or vice versa. If, for example, we choose $\mathbf{q}_c$ to be of the form $(\pi/a)(1,1,\xi)$ with $0\leq\xi\leq 1$, the quantity $\Gamma(\mathbf{q})$ is then a sharply peaked function of $\mathbf{q}$; so at least in this case certain sections of the Fermi surface may be regarded as being responsible for the instability of the paramagnetic state. For this restricted range of $\mathbf{q}_c$ the quantity $\epsilon_{\mathbf{k}+\mathbf{q}}-\epsilon_{\mathbf{k}}$ does not depend on $k_x$ or $k_y$ if $\mathbf{k}$ is required to lie on a constant energy surface so that one expects that a relatively large portion of Fermi surface will contribute to the instability. In the case of $n/N=1$ the whole Fermi surface contributes; as $n/N$ decreases the contributing portion of Fermi surface decreases until at $n/N=0.42$ the critical $\mathbf{q}_c$ is $(\pi/a)(1,1,0)$ and only that part of the Fermi surface near $k_z=0$ is important. Figure 4 shows cross sections of the Fermi surfaces corresponding to $n/N=1$ and $n/N=0.42$, and the related vectors $\mathbf{q}_c$ are also indicated. For $0.14<n/N<0.42$ we find that $\mathbf{q}_c$ has the form $\pi/a(1,\xi,0)$; $\xi$ decreases from one to zero as $n/N$ goes from 0.42 to 0.14. For $n/N<0.14$, we find $\mathbf{q}_c=0$ which means that the paramagnetic is unstable with respect to the ferromagnetic state.

It has been stated by Friedel *et al.*[15] that magnetism in the transition metals originates when the first local moments are formed on the individual atomic sites; subsequently, these moments are coupled through a sort of Ruderman-Kittel interaction involving the $d$ electrons themselves to give magnetic ordering. The

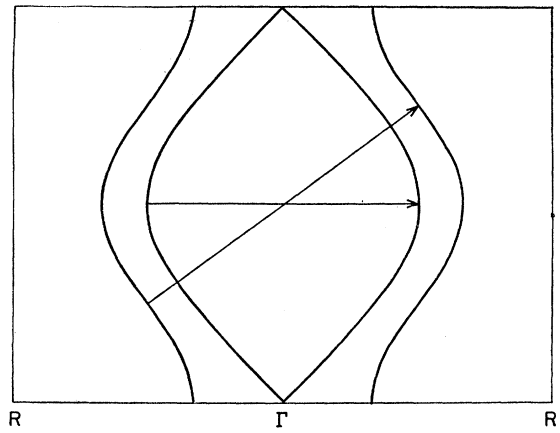


FIG. 4. Sections of the Fermi surface of the paramagnetic state in the [111] direction for the cases $n/N=1$ and $n/N=0.42$. The arrows represent $\mathbf{q}_c$ of Eq. (6.13).

condition for local moment formation is given as $C_0\eta_0(\epsilon_F)>1$ which then becomes the condition for magnetism itself. As stated by Friedel *et al.* themselves, it would be difficult with such a theory to explain the antiferromagnetism of Cr, which has a low $\eta_0(\epsilon_F)$; furthermore, Fig. 2 shows clearly that the condition $C_0\eta_0(\epsilon_F)>1$ is in general too restrictive. In the particular case of a half-filled band our model predicts magnetism for all $C_0$. For a more general band structure, the criterion involves, as we have stated above, a near correspondence between the magnetic zone structure and the unperturbed Fermi surface, rather than simply the density of states. The point of view adopted here is closer to those of Slater,[2] of des Cloiseaux,[8] and of Overhauser.[9]

## VII. FERROMAGNETIC STATE

The ferromagnetic state has the operator transformation [Eq. (4.3)] given by

$$\gamma_{k\uparrow}=a_{k\uparrow}, \tag{7.1a}$$

$$\gamma_{k\downarrow}=a_{k\downarrow}. \tag{7.1b}$$

The one-electron energies are [see Fig. 5(a)]

$$\epsilon_{k\uparrow}=\epsilon_k+A_{0\uparrow}, \tag{7.2a}$$

$$\epsilon_{k\downarrow}=\epsilon_k+A_{0\downarrow}, \tag{7.2b}$$

where

$$A_{0\uparrow}=C_0n_\downarrow/N, \tag{7.3a}$$

$$A_{0\downarrow}=C_0n_\uparrow/N, \tag{7.3b}$$

and

$$n_\sigma=\textstyle\sum_k F_{k\sigma}. \tag{7.4}$$

The total energy is

$$E=\textstyle\sum_{k\sigma} F_{k\sigma}\epsilon_k+A_{0\uparrow}A_{0\downarrow}N/C_0 \tag{7.5}$$

and the condition that the Fermi energy of the up-spin and down-spin bands be equal is

$$\epsilon_\downarrow-\epsilon_\uparrow=A_{0\uparrow}-A_{0\downarrow}, \tag{7.6}$$

where $\epsilon_\sigma$ is the Fermi energy of the spin-$\sigma$ band as measured with respect to the center of that band. Equation (7.6) tells us that the ferromagnetic state exists only above the line given by Eq. (6.9). The line along which the magnetization $M_z(0)$ is a fraction $\xi$ of the maximum possible value is plotted in Fig. 6. Above the line $\xi=1$, the ferromagnetic state is maximally polarized.

Both the paramagnetic response function and the actual energy comparison give the result that the ferromagnetic state lies lower in energy than the paramagnetic state in the region where both states exist. The additional kinetic energy necessary to form the ferromagnetic state is more than compensated for by the reduction in the repulsive energy between states of opposite spin. In the present model, and in the present case, the only role played by exchange is to cancel out the direct energy between parallel spins and, consequently, the exchange plays no role in determining the relative stability of the para- and ferromagnetic states. This remark, in fact, applies to all states except those containing spiral configurations where the exchange does play a different role.

The $x$ component of the ferromagnetic susceptibility evaluated at $\mathbf{q}=0$ is identically zero, reflecting the degeneracy of a ferromagnetic state quantized in the $z$ direction with any similar state quantized along a different axis. The susceptibility $\chi_z(0)$ is given by (A16) and is infinite if

$$(1/\eta_{0\uparrow})+(1/\eta_{0\downarrow})-2C_0=0, \tag{7.7}$$

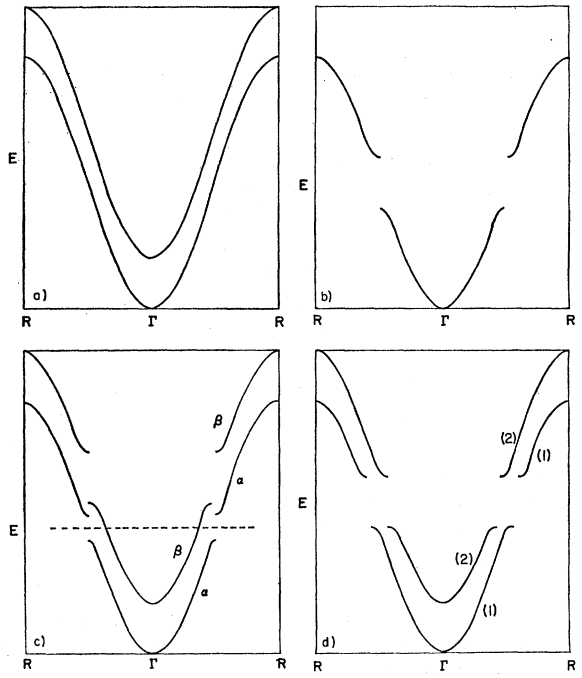


FIG. 5. The energy bands in the [111] direction for the following states: (a) ferromagnetic, (b) antiferromagnetic, (c) ferrimagnetic, (d) spiral-spin-density wave. The dashed line of (c) indicates the Fermi energy of a special ferrimagnetic state.

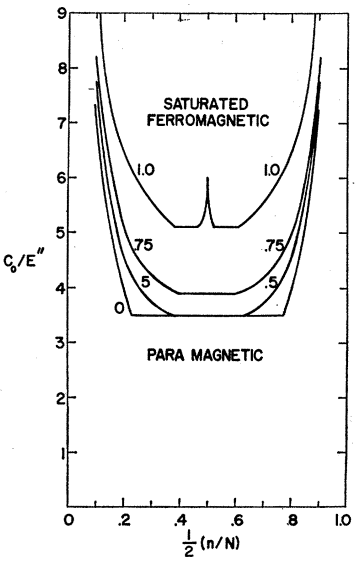


FIG. 6. The lines along which the magnetization of the ferromagnetic state is a given fraction of the maximum possible magnetization. The ferromagnetic state does not exist below the line indicating zero magnetization and is maximally magnetized above the line that indicates maximum magnetization.

where $\eta_{0\sigma}$ is the density of states of the spin $\sigma$ band at the Fermi energy. The line determined by (7.7) is line $a$ of Fig. 2.

The response function $\chi_x(\mathbf{Q})$ is found by using the method described in Sec. V

$$\chi_x(\mathbf{Q})=-2\mu_B{}^2\Gamma_{\uparrow\downarrow}(\mathbf{Q})/(1+C_0\Gamma_{\uparrow\downarrow}(\mathbf{Q})), \quad (7.8)$$

where

$$\Gamma_{\uparrow\downarrow}(\mathbf{Q})=(1/N)\textstyle\sum_{\mathbf{k}}(F_{\mathbf{k}+\mathbf{Q}\uparrow}-F_{\mathbf{k}\downarrow})/(\epsilon_{\mathbf{k}+\mathbf{Q}\uparrow}-\epsilon_{\mathbf{k}\downarrow}). \quad (7.9)$$

The quantity $\Gamma_{\uparrow\downarrow}(\mathbf{Q})$ can be rewritten as

$$\Gamma_{\uparrow\downarrow}(\mathbf{Q})=\int^{\epsilon F\uparrow} d\epsilon\,\eta_0(\epsilon)/[2\epsilon+C_0(n_\downarrow-n_\uparrow)] + \int^{\epsilon F\downarrow} d\epsilon\,\eta_0(\epsilon)/[2\epsilon-C_0(n_\downarrow-n_\uparrow)]. \quad (7.10)$$

The line $1/\chi_x(\mathbf{Q})=0$ is shown in Fig. 7 as line $a$. The susceptibility is negative in the region enclosed by the lines labeled $a$ and $c$.

The condition $1/\chi_z(\mathbf{Q})=0$ is from (A15)

$$1-C_0{}^2\int^{\epsilon F\downarrow} d\epsilon\,\eta_0(\epsilon)/\epsilon\int^{\epsilon F\uparrow} d\epsilon\,\eta_0(\epsilon)/\epsilon=0 \quad (7.11)$$

and this line is labeled $b$ in Fig. 7. Inside the small region bounded by the lines $b$ and $c$ we have $\chi_z(\mathbf{Q})<0$, and there the ferrimagnetic state lies lower in energy than the ferromagnetic state. The susceptibility becomes negative when the Fermi surface of one of the spin bands approaches the magnetic zone boundary. We recall that an instability in the paramagnetic state occurs when the Fermi surface of that state approaches the magnetic zone boundary; the present situation is a simple analog of the paramagnetic case.

## VIII. ANTIFERROMAGNETIC STATE

The antiferromagnetic state, quantized such that $M_z(\mathbf{Q})\neq 0$, is defined by

$$A_{0\uparrow}=A_{0\downarrow}=A_0, \quad (8.1a)$$

$$A_{Q\uparrow}=-A_{Q\downarrow}=A_Q. \quad (8.1b)$$

Diagonalizing the energy matrix of Eq. (4.6) yields two sets of operator transformations and one-electron energies

$$\gamma_{\mathbf{k}\uparrow}=aa_{\mathbf{k}\uparrow}+ba_{\mathbf{k}+\mathbf{Q}\uparrow}, \quad (8.2a)$$

$$E_{\mathbf{k}\uparrow}=A_0+\tfrac{1}{2}(\epsilon_{\mathbf{k}}+\epsilon_{\mathbf{k}+\mathbf{Q}})\pm[(\tfrac{1}{2}\epsilon_{\mathbf{k}+\mathbf{Q}}-\epsilon_{\mathbf{k}})^2+A_Q{}^2]^{1/2}, \quad (8.2b)$$

$$a=-A_Q/[A_Q{}^2+(\epsilon_{\mathbf{k}}-E_{\mathbf{k}\uparrow})^2]^{1/2}, \quad (8.2c)$$

and

$$\gamma_{\mathbf{k}\downarrow}=-aa_{\mathbf{k}\downarrow}+ba_{\mathbf{k}+\mathbf{Q}\downarrow}, \quad (8.2d)$$

$$E_{\mathbf{k}\downarrow}=E_{\mathbf{k}\uparrow}=E_{\mathbf{k}}. \quad (8.2e)$$

The energy band $E_{\mathbf{k}}$ is shown in Fig. 5(b). The total energy is, from (4.10),

$$E=\textstyle\sum_{\mathbf{k}\sigma}F_{\mathbf{k}\sigma}E_{\mathbf{k}}-(A_0{}^2-A_Q{}^2)(N/C_0), \quad (8.3)$$

where $F_{\mathbf{k}\sigma}$ is the occupation number of the eigenstate $\mathbf{k}\sigma$ defined in (8.2). Equations (4.5) yield

$$A_0=(C_0/N)\textstyle\sum_{\mathbf{k}}F_{\mathbf{k}\downarrow}=(C_0/N)\sum_{\mathbf{k}}F_{\mathbf{k}\uparrow}, \quad (8.4a)$$

$$A_Q=-2(C_0/N)\textstyle\sum_{\mathbf{k}}F_{\mathbf{k}\downarrow}ab. \quad (8.4b)$$

Because $\epsilon_{\mathbf{k}}=-\epsilon_{\mathbf{k}+\mathbf{Q}}$, we have

$$E_{\mathbf{k}}=A_0\pm(\epsilon_{\mathbf{k}}{}^2+A_Q{}^2)^{1/2} \quad (8.5)$$

and we see that the constant energy surface of the antiferromagnetic and paramagnetic states coincide. Equation (8.5) implies that the magnetic zone boundary is given by $\epsilon_{\mathbf{k}}=0$. For a half-filled band in the paramag-

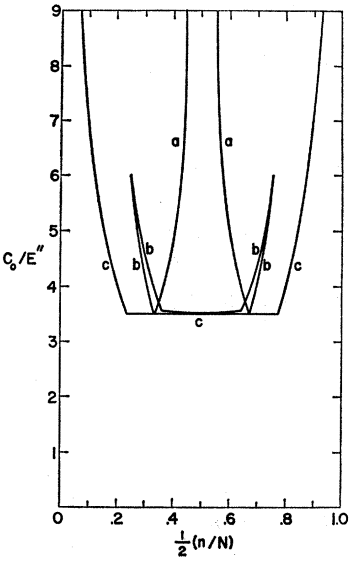


FIG. 7. The phase boundaries determined by an infinite value of the ferromagnetic susceptibility $\chi$ for the cases $\chi=\chi_x(\mathbf{Q})$ (line $a$), $\chi=\chi_z(\mathbf{Q})$ (line $b$), $\chi=\chi_z(0)$ (line $c$).

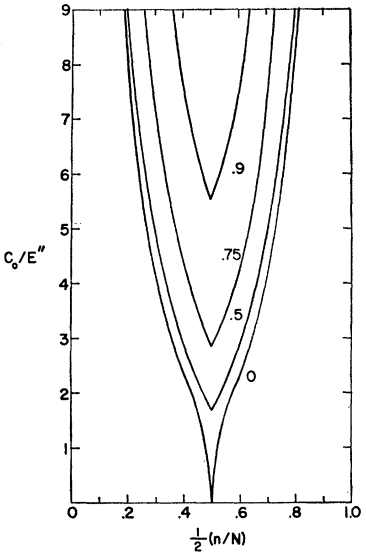


FIG. 8. The lines along which the magnetization $M_z(\mathbf{Q})$ of the antiferromagnetic state is a given fraction of the maximum possible magnetization. The antiferromagnetic state does not exist below the line corresponding to $M_z(\mathbf{Q})=0$.

netic case, $\epsilon_F=0$, the Fermi surface coincides with the magnetic zone boundary, the inner magnetic zone is completely filled, and consequently, the antiferromagnetic state is insulating for this particular valence even for vanishingly small interaction strength $C_0$. Of course, this extreme result is a special feature of the present model; for a more general band structure, however, particular valences can be expected to exist for which there is a maximal reduction of the area of the Fermi surface upon transition from the paramagnetic to the antiferromagnetic state when the theoretical strength of interaction is reached. For still larger values of $C_0$, one may expect the antiferromagnetic state to become insulating. In this connection, it is interesting to note the remarks of Griffith and Coles[17] concerning $\alpha$-Mn and those of Lomer[18] concerning Cr which support the present point of view strongly.

Equations (8.3) and (8.4) take the form

$$E=2\int^{\epsilon_F}[A_0\pm(\epsilon^2+A_Q^2)^{1/2}]\eta_0(\epsilon)d\epsilon - (A_0^2-A_Q^2)(N/C_0), \quad (8.6)$$

$$A_0=\tfrac{1}{2}C_0n/N, \quad (8.7)$$

$$A_Q=A_Q(C_0/N)\int^{\epsilon_F}d\epsilon\,\eta_0(\epsilon)/[\mp(A_Q^2+\epsilon^2)^{1/2}]. \quad (8.8)$$

The nontrivial solution for $A_Q$ determined by

$$1=(C_0/N)\int^{\epsilon_F}d\epsilon\,\eta_0(\epsilon)/[\mp(A_Q^2+\epsilon^2)^{1/2}] \quad (8.9)$$

gives the size of the band gap and the magnitude of $M_z(\mathbf{Q})$. The antiferromagnetic state exists in the region above the line given by (6.12) (see Fig. 2); (8.9) reduces to (6.10) in the limit $A_Q\to 0$. In Fig. 8 we have drawn lines of constant $\xi$ where $\xi$ is defined as the ratio of actual magnetization of the antiferromagnetic state to maximum possible magnetization for a given $n$.

The antiferromagnetic state has a lower energy than the paramagnetic state in the region of the phase diagram in which both states exist, as may be seen directly from (6.4), (8.6) and (8.9). In Fig. 9, we have indicated the state of lowest energy among the paramagnetic, ferromagnetic, and antiferromagnetic states. The solid lines indicate a second-order transformation. The dashed lines indicate a first-order transformation and are determined by a calculation of the appropriate energies. At a point in the phase diagram where all three states exist, the energies of the states satisfy

$$\text{E.B.)}_{\text{Para}}<\text{E.B.)}_{\text{Anti}}<\text{E.B.)}_{\text{Ferro}}, \quad (8.10a)$$

$$\text{E.I.)}_{\text{Para}}>\text{E.I.)}_{\text{Anti}}>\text{E.I.)}_{\text{Ferro}}, \quad (8.10b)$$

where E.B. represents the band energy, and E.I. represents the total spin-dependent interaction energy.

The quantity $\chi_x(0)$, the $x$ component of the antiferromagnetic susceptibility, is found using the method outlined in Sec. V:

$$\chi_x(0)=-2\mu_B^2(A+B)/(1+C_0A+C_0B), \quad (8.11)$$

where

$$A=\epsilon_F\eta_0(\epsilon_F)/[\mp(\epsilon_F^2+A_Q^2)^{1/2}], \quad (8.12)$$

and

$$B=A_Q^2\int^{\epsilon_F}d\epsilon\,\eta_0(\epsilon)/[\pm(\epsilon^2+A_Q^2)^{3/2}]. \quad (8.13)$$

The susceptibility $\chi_x(0)$ is positive in regions 2 and 3 of

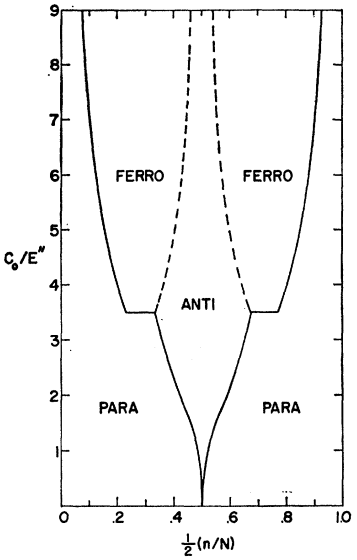


FIG. 9. The phase diagram for the paramagnetic, antiferromagnetic, and ferromagnetic states. The region of phase space in which each state is stable is indicated. Solid lines indicate second-order phase transformations and dashed lines indicate first-order transformations.

[17] D. Griffith and B. R. Coles, Proc. Phys. Soc. (London) 82, 127 (1963).
[18] W. M. Lomer, Proc. Phys. Soc. (London) 80, 489 (1962).

TABLE III. States which may transform into one another at the second-order phase boundaries shown in Fig. 11.

| Phase boundary line | |
|---|---|
| *a* | paramagnetic, antiferromagnetic |
| *b* | paramagnetic, ferromagnetic |
| *c* | antiferromagnetic, ferrimagnetic |
| *d* | ferromagnetic, ferrimagnetic |
| *e* | antiferromagnetic, SSDW |
| *f* | ferromagnetic, SSDW |

Fig. 10 and is negative in region 1. Thus, in region 1, the antiferromagnetic state is unstable. The quantity $1/\chi_x(\mathbf{Q})$ is identically zero indicating that the antiferromagnetic state with $M_z(\mathbf{Q})$ nonzero is degenerate with any antiferromagnetic state obtained from it by rotation of the direction of magnetization.

The quantity $\chi_z(0)$ can be shown to be

$$\chi_z(0)=-2\mu_B^2(2+C)/[(2+C)(C_0+D)-F], \quad (8.14)$$

where

$$C=C_0A_Q^2\int^{\epsilon_F} d\epsilon\,\eta_0(\epsilon)/[\pm(\epsilon^2+A_Q^2)^{3/2}], \quad (8.15a)$$

$$D=\epsilon_F/[\mp(\epsilon_F^2+A_Q^2)^{1/2}\eta_0(\epsilon_F)], \quad (8.15b)$$

$$F=C_0A_Q^2/(\epsilon_F^2+A_Q^2). \quad (8.15c)$$

We find that $\chi_z(0)$ is positive in region 3 and negative in regions 1 and 2 of Fig. 10.

We have summarized the information contained in the expression $(1/\chi)=0$ in Fig. 11 and Table III. Each entry in the table corresponds to a second-order phase boundary in Fig. 11 and indicates which two states co-exist on the boundary.

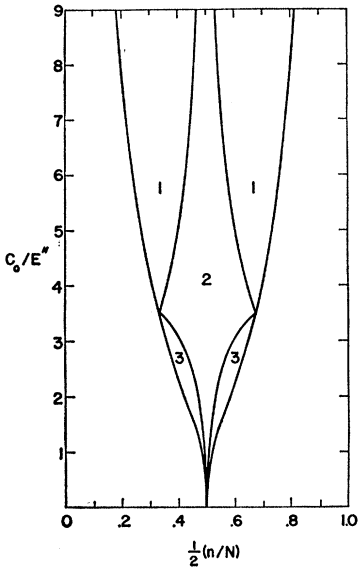


FIG. 10. The sign of the $x$ and $z$ components of the $\mathbf{q}=0$ antiferromagnetic susceptibility: $\chi_x$ is negative in region 1 and positive in regions 2 and 3; $\chi_z$ is positive in region 3 and negative in regions 1 and 2.

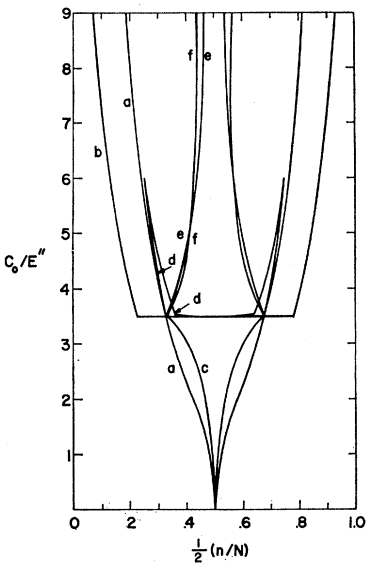


FIG. 11. The phase boundaries determined by $1/\chi=0$ where $\chi$ is the $\mathbf{q}=\mathbf{Q}$ or the $\mathbf{q}=0$ paramagnetic susceptibility (line *a* and line *b*, respectively), the $\mathbf{q}=0$ $z$ component of the antiferromagnetic susceptibility (line *c*), the $\mathbf{q}=\mathbf{Q}$ $z$ component of the ferromagnetic susceptibility (line *d*), the $\mathbf{q}=0$ $x$ component of the antiferromagnetic susceptibility (line *e*), the $\mathbf{q}=\mathbf{Q}$ $x$ component of the ferromagnetic susceptibility (line *f*).

## IX. FERRIMAGNETIC STATE

The ferrimagnetic state is defined by

$$A_{0\uparrow}\neq A_{0\downarrow}, \quad (9.1a)$$

$$A_{Q\uparrow}\neq -A_{Q\downarrow}. \quad (9.1b)$$

Equations (4.9) give

$$M_z(0)=(\mu_B/C_0)(A_{0\downarrow}-A_{0\uparrow}), \quad (9.2a)$$

$$M_z(\mathbf{Q})=(\mu_B/C_0)(A_{Q\downarrow}-A_{Q\uparrow}), \quad (9.2b)$$

$$n(\mathbf{Q})=(1/C_0)(A_{Q\downarrow}+A_{Q\uparrow}). \quad (9.2c)$$

The charge fluctuation indicated by (9.2c) implies a nonzero net charge within an atomic cell which would create a large perturbation on a neighboring cell. In this case, the neglect of interactions on different cells is not justifiable. To include them would, however, greatly complicate the calculations; we shall leave the problem for future study, bearing in mind that the present results are subject to quantitative revision. The diagonalization of the energy matrix of (4.6) leads to the operator transformation and eigenvalues

$$\gamma_{k\uparrow}=c_\uparrow a_{k\uparrow}+d_\uparrow a_{k+Q\uparrow}, \quad (9.3a)$$

$$E_{k\uparrow\pm}=A_{0\uparrow}\pm(\epsilon_k^2+A_{Q\uparrow}^2)^{1/2}, \quad (9.3b)$$

$$c_\uparrow=-A_{Q\uparrow}/[A_{Q\uparrow}^2+(\epsilon_k-E_{k\uparrow})^2]^{1/2}. \quad (9.3c)$$

The plus sign of (9.3b) is chosen when $\epsilon_k>0$. There are exactly analogous expressions for $\gamma_{k\downarrow}$, $E_{k\downarrow\pm}$ and $c_\downarrow$. The energy bands described by Eq. (9.3b) are shown in Fig. 5(c). One can imagine the bands as being formed by the application of periodic potentials of strengths $A_{Q\downarrow}$ and $A_{Q\uparrow}$ to the ferromagnetic state depicted in Fig. 5(a).

There is a particular ferrimagnetic state of great importance because it is the state of lowest energy over a wide region of the phase diagram, whereas the general

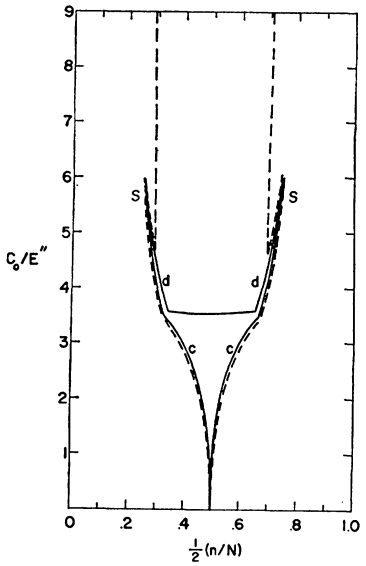


FIG. 12. The ferrimagnetic state exists only within the region bounded by the dashed curve. The special ferrimagnetic state exists everywhere in that region while the general ferrimagnetic state does not exist in the region bounded by the curves $c$ and $d$.

ferrimagnetic state is never a state of lowest energy. This particular state, which we shall refer to as the special ferrimagnetic (S.F.) state is described in the case $n<1$, $\epsilon_F<0$ by

$$n=\tfrac{1}{2};\ \text{(lower half-band of spin-down filled)} \tag{9.4a}$$

$$E_{F\uparrow -}<E_{F\downarrow}<E_{F\uparrow +}. \tag{9.4b}$$

The Fermi level of such a S.F. state is indicated by the dashed line in Fig. 5(c). There is, of course, a similar S.F. state with $n>1$. Notice that in the case $n=1$, the S.F. state becomes identical to the antiferromagnetic state.

In general, for all ferrimagnetic states, (4.6) and (9.3) lead to

$$A_{0\uparrow}=C_0 n_\downarrow/N, \tag{9.5a}$$

$$A_{0\downarrow}=C_0 n_\uparrow/N, \tag{9.5b}$$

and

$$A_{Q\uparrow}=C_0 A_{Q\downarrow}\int^{\epsilon_{F\downarrow}} d\epsilon\ \eta_0(\epsilon)/[\pm(\epsilon^2+A_{Q\downarrow}{}^2)^{1/2}], \tag{9.6a}$$

$$A_{Q\downarrow}=C_0 A_{Q\uparrow}\int^{\epsilon_{F\uparrow}} d\epsilon\ \eta_0(\epsilon)/[\pm(\epsilon^2+A_{Q\uparrow}{}^2)^{1/2}], \tag{9.6b}$$

where $\epsilon_{F\sigma}$ corresponds to the Fermi energy of spin-$\sigma$ electrons. In the case of the S.F. state, we have $\epsilon_{F\uparrow}=0$. The condition that the actual Fermi energies be equal, $E_{F\uparrow}=E_{F\downarrow}$, gives

$$A_{0\uparrow}\pm(\epsilon_{F\uparrow}{}^2+A_{Q\uparrow}{}^2)^{1/2}=A_{0\downarrow}\pm(\epsilon_{F\downarrow}{}^2+A_{Q\downarrow}{}^2)^{1/2}, \tag{9.7}$$

while in the case of the S.F. state, (9.4) replaces (9.7). Equations (9.6) and (9.7) constitute three equations which for a given $C_0$ and $n$ are sufficient to determine $A_{Q\uparrow}$, $A_{Q\downarrow}$, $A_{0\uparrow}$, $A_{0\downarrow}$, $\epsilon_{F\uparrow}$ and $\epsilon_{F\downarrow}$, the last three quantities being determined by the first three, since $A_{0\downarrow}=C_0 n-A_{0\uparrow}$ and $\epsilon_{F\uparrow}$ is determined by $n_\uparrow$.

The most convenient method for solving the simultaneous equations (9.6) and (9.7) is as follows. First eliminate $C_0$ from equations (9.6) with the result

$$A_{Q\downarrow}{}^2\int^{\epsilon_{F\downarrow}} d\epsilon\ \eta_0(\epsilon)/[\pm(\epsilon^2+A_{Q\downarrow}{}^2)^{1/2}] = A_{Q\uparrow}{}^2\int^{\epsilon_{F\uparrow}} d\epsilon\ \eta_0(\epsilon)/[\pm(\epsilon^2+A_{Q\uparrow}{}^2)^{1/2}]. \tag{9.8}$$

The integral $I(\epsilon_F,A)$ defined by

$$I(\epsilon_F,A)=A^2\int^{\epsilon_F} d\epsilon\ \eta_0(\epsilon)/[\pm(\epsilon^2+A^2)^{1/2}] \tag{9.9}$$

is then plotted as a function of $\epsilon_F$ for various values of $A$. We now specify values for $A_{Q\uparrow}$ and $\epsilon_{F\uparrow}$ instead of specifying $C_0$ and $n$. Equation (9.8) then defines a set of possible combinations of values for $\epsilon_{F\downarrow}$ and $A_{Q\downarrow}$. One pair from this set is picked, and then $C_0$ is determined from Eq. (9.6a). We then can see whether (9.7) is satisfied, if it is not, we try a different pair of values for $\epsilon_{F\uparrow}$ and $A_{Q\uparrow}$. In the S.F. case, we follow the same procedure except that we must choose $\epsilon_{F\uparrow}=0$, and, after we have found $\epsilon_{F\downarrow}$ and $A_{Q\downarrow}$, we check to see if (9.4b) is satisfied.

The S.F. state exists everywhere within the region bounded by the dashed curve of Fig. 12. The spikes, labeled $S$ in the figure, were put in by hand as they are too narrow to be found by the numerical procedure but are indicated by the fact that the $z$ component of the $\mathbf{q}=\mathbf{Q}$ ferromagnetic susceptibility is negative in that region. The lines $c$ and $d$ of Fig. 12 are the lines $c$ and $d$ of Fig. 11. The general ferrimagnetic state exists outside the closed region bounded by the lines $c$ and $d$ and within the region bounded by the dashed curve. On the dashed curve of Fig. 12, the S. F. state becomes a limiting case of the ferrimagnetic state in the sense that the Fermi level just touches the top of the down-spin sub-band.

The S.F. state and the antiferromagnetic state have nearly the same energy near the region where $n\sim 1$ with the S.F. state always having a slightly lower energy. Thus, the line determined by $E_{\text{ferro}}=E_{\text{S.F.}}$ lies very close to the line $E_{\text{ferro}}=E_{\text{anti}}$, particularly for large $C_0$ (i.e., for $n\sim 1$). Figure 13 indicates the state of lowest energy among the paramagnetic, ferromagnetic, antiferromagnetic, and ferrimagnetic states. The dashed lines indicate first-order phase transformations and the solid lines indicate second-order phase transformations.

## X. SPIRAL-SPIN-DENSITY-WAVE STATE AND FINAL-PHASE DIAGRAM

The spiral-spin-density-wave state is defined by

$$A_{0\uparrow}\neq A_{0\downarrow}, \tag{10.1a}$$

$$A_{Q\uparrow\downarrow}=A_Q\neq 0, \tag{10.1b}$$

and Eqs. (4.9) give

$$M_z(0)=(\mu_B/C_0)(A_{0\downarrow}-A_{0\uparrow}), \tag{10.2a}$$

$$M_x(Q)=-(2\mu_B/C_0)A_Q, \tag{10.2b}$$

together with no charge density fluctuation. The eigenvalues and operator transformation determined from diagonalizing the energy matrix are

$$\gamma_{\mathbf{k}}^{(1)}=e^{(1)}a_{\mathbf{k}\downarrow}+f^{(1)}a_{\mathbf{k}+\mathbf{Q}\uparrow}, \tag{10.3a}$$

$$E_{\mathbf{k}}^{(1)}=A_{0+}\pm[(\epsilon_{\mathbf{k}}-A_{0-})^2+A_Q^2]^{1/2}, \tag{10.3b}$$

$$e^{(1)}=-A_Q[(\epsilon_{\mathbf{k}}+A_{0\downarrow}-E_{\mathbf{k}}^{(1)})^2+A_Q^2]^{-1/2}, \tag{10.3c}$$

$$\gamma_{\mathbf{k}}^{(2)}=f^{(2)}a_{\mathbf{k}\uparrow}+e^{(2)}a_{\mathbf{k}+\mathbf{Q}\downarrow}, \tag{10.3d}$$

$$E_{\mathbf{k}}^{(2)}=A_{0+}\pm[(\epsilon_{\mathbf{k}}+A_{0-})^2+A_Q^2]^{1/2}, \tag{10.3e}$$

$$f^{(2)}=-A_Q[(\epsilon_{\mathbf{k}}+A_{0\uparrow}-E_{\mathbf{k}}^{(2)})^2+A_Q^2]^{-1/2}, \tag{10.3f}$$

where

$$A_{0+}=\tfrac{1}{2}(A_{0\uparrow}+A_{0\downarrow}), \tag{10.4a}$$

$$A_{0-}=\tfrac{1}{2}(A_{0\uparrow}-A_{0\downarrow}), \tag{10.4b}$$

the minus sign in (10.3b) is chosen if $\epsilon_{\mathbf{k}}-A_{0-}<0$, and the minus sign in Eq. (10.3e) is chosen if $\epsilon_{\mathbf{k}}+A_{0-}<0$. The one-electron energy versus $\mathbf{k}$ curves are shown in Fig. 5(d). The form of the energy bands in the figure may be imagined as the result of applying to a ferromagnet a periodic potential of strength $A_Q$ that mixes states of opposite spin.

Equations (4.5) give

$$A_{0\uparrow}=(C_0/N)\sum_{\mathbf{k},i=1}^{2}F_{\mathbf{k}}^{(i)}(e^{(i)})^2, \tag{10.5a}$$

$$A_{0\downarrow}=(C_0/N)\sum_{\mathbf{k},i=1}^{2}F_{\mathbf{k}}^{(i)}(f^{(i)})^2, \tag{10.5b}$$

$$A_Q=-(C_0/N)\sum_{\mathbf{k},i=1}^{2}F_{\mathbf{k}}^{(i)}e^{(i)}f^{(i)}, \tag{10.5c}$$

where $F_{\mathbf{k}}^{(i)}$ is the occupation number of the state $\mathbf{k}(i)$ defined by (10.3). Note that the number of electrons of spin-up is given by

$$n_\uparrow=\sum_{\mathbf{k},i=1}^{2}F_{\mathbf{k}}^{(i)}(f^{(i)})^2, \tag{10.6}$$

so that

$$A_{0\downarrow}=C_0n_\uparrow/N \tag{10.7}$$

as usual, but that the number of electrons in band $(i)$ is given by

$$n^{(i)}=\textstyle\sum_{\mathbf{k}}F_{\mathbf{k}}^{(i)}, \tag{10.8}$$

which is not the same as the number of spin-down or spin-up electrons in band $(i)$. With the help of (10.3c) and (10.3f), (10.5c) can be put in the form

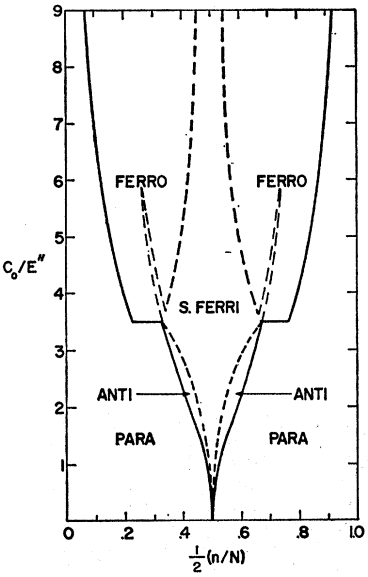


FIG. 13. The phase diagram for the paramagnetic, ferromagnetic, antiferromagnetic, and ferrimagnetic states. Solid lines indicate second-order phase transformations and dashed lines indicate first-order transformations.

$$1=\tfrac{1}{2}C_0\int^{\epsilon_F^{(1)}}d\epsilon\,\eta_0(\epsilon)/\{\mp[(\epsilon-A_{0-})^2+A_Q^2]^{1/2}\}$$

$$+\tfrac{1}{2}C_0\int^{\epsilon_F^{(2)}}d\epsilon\,\eta_0(\epsilon)/\{\mp[(\epsilon+A_{0-})^2+A_Q^2]^{1/2}\}. \tag{10.9}$$

The condition $E_F^{(1)}=E_F^{(2)}$ yields

$$\pm[(\epsilon_F^{(1)}-A_{0-})^2+A_Q^2]^{1/2}=\pm[(\epsilon_F^{(2)}+A_{0-})^2+A_Q^2]^{1/2}. \tag{10.10}$$

On using Eqs. (10.3c), (10.3f), and (10.5c) to evaluate $A_{0-}$, we find that

$$A_{0-}=\tfrac{1}{2}C_0\int^{\epsilon_F^{(1)}}d\epsilon\,\eta_0(\epsilon)(\epsilon-A_{0-})/\{\pm[(\epsilon-A_{0-})^2+A_Q^2]^{1/2}\}-\tfrac{1}{2}C_0\int^{\epsilon_F^{(2)}}d\epsilon\,\eta_0(\epsilon)\times(\epsilon+A_{0-})/\{\pm[(\epsilon+A_{0-})^2+A_Q^2]^{1/2}\}. \tag{10.11}$$

Combining Eqs. (10.9) and (10.11) yields

$$0=\int^{\epsilon_F^{(1)}}d\epsilon\,\eta_0(\epsilon)\epsilon/\{\pm[(\epsilon-A_{0-})^2+A_Q^2]^{1/2}\}-\int^{\epsilon_F^{(2)}}d\epsilon\,\eta_0(\epsilon)\epsilon/\{\pm[(\epsilon+A_{0-})^2+A_Q^2]^{1/2}\}. \tag{10.12}$$

Equations (10.9), (10.10), and (10.12) are the three simultaneous equations that must be satisfied by the spiral-spin-density state. The use of Eqs. (4.10), (10.3b), (10.3c), and (10.7) results in an expression for

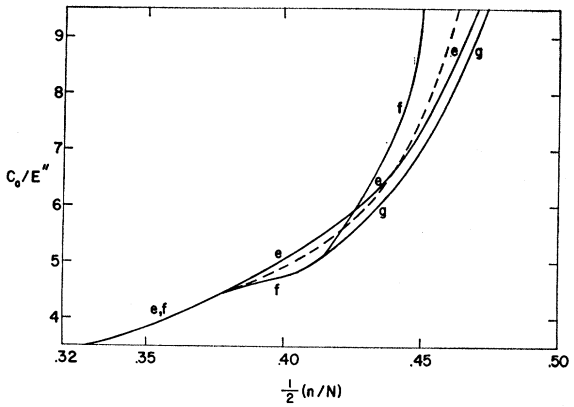


FIG. 14. The ferromagnetic susceptibility $\chi_x(\mathbf{Q})$ is infinite on line $f$. The antiferromagnetic suscepbility $\chi_x(0)$ is infinite on line $e$. The special spiral-spin-density-wave state exists in the region bounded by lines $f$ and $g$. The general spiral-spin-density-wave state exists in the region bounded by line $e$ and line $g$ above $C_0/E''=5.1$ and lines $e$ and $f$ below $C_0/E''=5.1$. The dashed curve indicates the first-order phase boundary separating the ferromagnetic and the antiferromagnetic states.

the total energy of the state

$$E=\int^{\epsilon_F^{(1)}} d\epsilon\,\eta_0(\epsilon)\{\pm[(\epsilon-A_{0-})^2+A_Q^2]^{1/2}\}+\int^{\epsilon_F^{(2)}} d\epsilon\,\eta_0(\epsilon)\{\pm[(\epsilon+A_{0-})^2+A_Q^2]^{1/2}\}+\tfrac{1}{2}C_0n^2/N-C_0n_\uparrow n_\downarrow/N+A_Q^2/C_0. \quad (10.13)$$

There is a special case of the spiral-spin-density-wave state (SSSDW) that is analogous to the S.F. state. Like the S.F. state, the SSSDW is the state of lowest energy in some regions of phase space but the general SSDW state never is. The SSSDW state can exist only when the quantity $A_{0-}$ is sufficiently large and consists of all the electrons being in one band. When $2A_{0-}$ is larger than the band width (i.e., $A_{0-}>3$), the periodic potential does not split the bands so that if $n<1$ then all the electrons will be in one band. Further, it is possible to have a band splitting and still have all the electrons in one band. The condition for this to happen is found from (10.3b) and (10.3e) to be

$$\epsilon_F^{(1)}\leq A_{0-}\leq 3, \quad (10.14)$$

where band (1) holds all $n$ electrons.

The self-consistency equations for the SSSDW state are

$$1=\tfrac{1}{2}C_0\int^{\epsilon_F^{(1)}} d\epsilon\,\eta_0(\epsilon)/\{\mp[(\epsilon-A_{0-})^2+A_Q^2]^{1/2}\}, \quad (10.15a)$$

$$0=\int^{\epsilon_F^{(1)}} d\epsilon\,\eta_0(\epsilon)\epsilon/\{\mp[(\epsilon-A_{0-})^2+A_Q^2]^{1/2}\}. \quad (10.15b)$$

In the limit $A_Q\to 0$, the SSSDW state will be degenerate with the maximally saturated ferromagnetic state along the line determined by $1/\chi_x(\mathbf{Q})=0$ where $\chi$ is the ferromagnetic susceptibility. Equations (10.15) are easily solved numerically by specifying values of $A_{0-}$ and $A_Q$ and then by using (10.15b) to determine $\epsilon_F^{(1)}$, i.e., $n$. The quantity $C_0$ is found by means of (10.15a) and a further check insures that $\epsilon_F^{(1)}<A_{0-}$. For a given $A_{0-}$, we can vary the value of $A_Q$ and generate a set of points on the phase diagram; as we increase $A_Q$ both $C_0$ and $n$ will increase.

As we have already noted, a SSSDW state with $A_Q=0$ corresponds to a maximally saturated ferromagnetic state; the line of such states is shown as line $f$ for $C_0>5.1$ in Fig. 14. If $A_{0-}>3$, then $\epsilon_F^{(1)}<A_{0-}$ for all $A_Q$. On the other hand, if $A_{0-}<3$, there will be some critical value for $A_Q$ such that the quantity $\epsilon_F^{(1)}$ generated by that $A_Q$ satisfies $\epsilon_F^{(1)}=A_{0-}$. These points will lie on a line that corresponds to the set of solutions of (10.9), (10.10), and (10.12) solved under the assumption $n^{(1)}=n$, $n^{(2)}=0$. This line is denoted by $g$ in Fig. 14. The SSSDW state exists in the region bounded by the lines $f$ and $g$ in Fig. 14 above $C_0=5.1$. As is expected from the fact that the ferromagnetic susceptibility is negative in this region, the energy of the SSSDW state lies below that of the ferromagnetic state.

We now take up the problem of constructing the more general SSDW state. The three simultaneous equations (10.9), (10.10), and (10.12) can be dealt with as follows. We first choose values for $n^{(1)}$ and $n^{(2)}$, and then use Eq. (10.10) to find $A_{0-}$. Next $A_Q$ can be determined from (10.12) via a trial and error procedure. Finally, $C_0$ is found from Eq. (10.9).

The case $n^{(1)}=n^{(2)}=n/2$ corresponds to a point at which this SSDW state is degenerate with the antiferromagnetic state, which occurs along the line $e$ of Figs. 11 and 14. This line is determined by the condition $1/\chi_x(0)=0$ where $\chi_x(0)$ is the antiferromagnetic susceptibility. For a fixed value of $n$, as $n^{(1)}-n^{(2)}$ increases

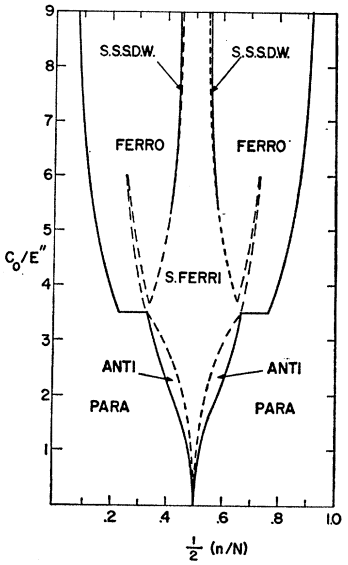


FIG. 15. The phase diagram for the paramagnetic, ferromagnetic, antiferromagnetic, ferrimagnetic, and spiral-spin-density-wave states. Solid lines indicate second-order phase transformations and dashed lines indicate first-order transformations.

the SSDW state exists towards lower values of $C_0$. In the case of $n$ sufficiently large ($C_0>5.1$), we can increase the difference $n^{(1)}-n^{(2)}$ until it is equal to $n$ and still find a solution of the three simultaneous equations. As already discussed, the values of our parameters also satisfy (10.15) and can alternatively be constructed by using the method previously employed in constructing the SSSDW state, thus providing a check on the accuracy of the numerical procedures.

For $C_0<5.1$ there will be some maximum value of $n^{(1)}-n^{(2)}$ such that it is smaller than $n$ and still satisfies the simultaneous equations. This line of maximum $n^{(1)}-n^{(2)}$ is represented by the line $f$ below $C_0=5.1$ in Fig. 14. The SSDW state exists in the region between lines $e$ and $g$ for $C_0>5.1$ and between lines $e$ and $f$ for $C_0<5.1$. This state always has an energy greater than the antiferromagnetic state. The dashed line in Fig. 14 indicates the line at which the energy of the antiferromagnetic state is equal to the energy of the ferromagnetic tsate.

The final-phase diagram is shown in Fig. 15. The state of lowest energy is indicated, and second-order phase transformations are denoted as before by solid lines, while first-order transformations are indicated by dashed lines. We see that for the case of a half-filled band the special ferrimagnetic state is the state of lowest energy. As the number of electrons increases or decreases, the paramagnetic, antiferromagnetic, and ferromagnetic states become possible ground states depending on the value of $C_0/E''$. Finally, when the band is almost full or almost empty, only the paramagnetic state exists for not too large values of $C_0/E''$.

## XI. LOCAL MOMENTS

When an impurity atom is placed in a paramagnetic metal a local magnetic moment may be formed at the impurity site. This phenomenon has been treated by Wolff[11] and Clogston *et al.*[19] within the context of a model that is similar to ours. The Hamiltonian for the system of metal plus impurity potential takes the form

$$\langle 0\sigma|H|0\sigma'\rangle=\delta_{\sigma,\sigma'}(\langle 0\sigma|H_0|0\sigma\rangle+V_I+C_0\textstyle\sum_s\langle 0s|\Delta\rho|0s\rangle-C_0\langle 0\sigma|\Delta\rho|0\sigma\rangle), \quad (11.1a)$$

$$\langle l\sigma|H|l'\sigma'\rangle=\delta_{l,0}\delta_{l',0}\langle 0\sigma|H|0\sigma'\rangle+(1-\delta_{l,0}\delta_{l',0})\langle l\sigma|H_0|l'\sigma'\rangle, \quad (11.1b)$$

in first quantization, where $|l\sigma\rangle$ denotes a Wannier function of spin $\sigma$, $V_I$ represents the impurity potential, $\Delta\rho$ is the change in the density matrix induced by $V_I$, and $H_0$ is the unperturbed Hamiltonian. Equation (11.1) can be solved exactly for $\langle 0\sigma|\Delta\rho|0\sigma\rangle$ and a local moment is obtained when $\langle 0\uparrow|\Delta\rho|0\uparrow\rangle\neq\langle 0\downarrow|\Delta\rho|0\downarrow\rangle$. On solving for $\langle 0\sigma|\Delta\rho|0\sigma\rangle$, one finds that for a given valence of the host material there is a critical value of $C_0$, $C_0'$, such that if $C_0<C_0'$ no local moment is formed, independent of the size of $V_I$. For $C_0>C_0'$, there is a range of values of $V_I$ such that a local moment is formed. The line $C_0'=C_0'(n)$ has been plotted on the phase diagram and is the lower dashed line of Fig. 16. The line is meaningful only in those regions of phase space in which the ground state is paramagnetic as this was taken to be the state of the host metal when Eq. (11.1) was solved.

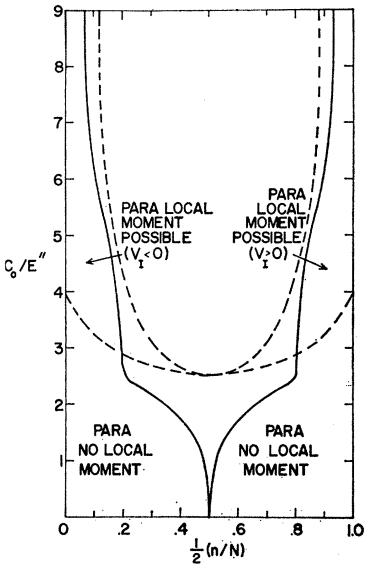


FIG. 16. The phase diagram describing the properties of the paramagnetic state with respect to local moment formation. Below the lower dashed curve no local moment can be formed independent of the strength of the impurity potential. Between the two dashed curves local moment formation is possible depending on the strength and sign of the impurity potential. Above the upper dashed curve local moments form in the absence of an impurity. The solid line indicates the phase boundary of the paramagnetic state (see Fig. 3).

For sufficiently large $C_0$ a local moment is formed in the case $V_I=0$; this indicates an instability of the host metal. The condition for this instability to occur may be found by examining the sign of the local susceptibility $\chi_{xl}=M_{xl}/H_{xl}$. This quantity is easily evaluated by means of the method described in Sec. V and is

$$\chi_{xl}=-2\mu_B^2\textstyle\sum_q\Gamma(\mathbf{q})/(1+C_0\sum_q\Gamma(\mathbf{q})), \quad (11.2)$$

where

$$\Gamma(\mathbf{q})=(1/N)\textstyle\sum_k(F_{k+q}-F_k)/(\epsilon_{k+q}-\epsilon_k). \quad (11.3)$$

The line in phase space corresponding to $1/\chi_{xl}=0$ is found from $0=1+C_0\sum_q\Gamma(\mathbf{q})$ which may be put in the form

$$0=1+2C_0\int_{-\infty}^{\epsilon_F}I(z)\eta_0(z)dz, \quad (11.4)$$

where

$$I(z)=P\int_{-\infty}^{\infty}dz'\eta_0(z')/(z-z') \quad (11.5)$$

and $P$ indicates that the principal part is to be taken. The line $1/\chi_{xl}=0$ is shown in Fig. 16 as the upper of the two dashed lines. The entire line is seen to lie within a region in which the paramagnetic state is unstable, as it should be since stability against a spontaneous local moment is less stringent than stability against an arbitrary polarization.

[19] A. M. Clogston, B. T. Matthias, M. Peter, M. J. Williams, E. Corenzwit, and R. C. Sherwood, Phys. Rev. **125**, 541 (1962).

## XII. CONCLUSION

We have given a semiquantitative explanation of the incidence and type of magnetism observed in the transition metals and alloys based on a SCF band model. The model contains two parameters; the number of electrons per atom $n/N$ and the strength of interaction between electrons compared to the bandwidth $C_0/E''$. The correlation between the values of the parameters and the position of a metal in the periodic table has been discussed; $n/N$ is directly related to the average atomic valence apart from the number of $s$ electrons and $C_0/E''$ is a quantity which is expected to increase strongly as one moves upward and to the right in the periodic table. For given values of the parameters there will be one or more types of magnetic states that may be constructed within the context of the model and we have been specifically interested in determining the state of lowest energy.

The region of phase space in which the paramagnetic state is stable against a second-order phase transformation to an antiferromagnetic or ferromagnetic state has been determined by a calculation of the paramagnetic susceptibility $\chi(\mathbf{q})$. Figure 3 shows the phase boundary at which the paramagnetic state becomes unstable and the upper portion of the figure gives the wave-number $\mathbf{q}_c$ for which the instability occurs. For $n/N=1$ the whole Fermi surface contributes to the instability, as $n/N$ decreases the area of the Fermi surface that contributes to the instability decreases until at $n/N=0.42$ only a narrow ring of the Fermi surface contributes as is shown in Fig. 4. As $n/N$ decreases still further, it is less justifiable to associate the instability with a particular portion of the Fermi surface. For $n/N<0.14$, we find $\mathbf{q}_c=0$.

Our primary concern has been in determining for a given $n/N$ and $C_0/E''$ the state of lowest energy among a limited number of the infinitely many states that may exist. The states chosen for study were the paramagnetic, ferromagnetic, antiferromagnetic, ferrimagnetic, and spiral-spin-density-wave states [the latter three states are characterized by a spatial variation of magnetization corresponding to $\mathbf{q}=(\pi/a)(1,1,1)$]. The phase diagram associated with these states have been constructed by means of the response function method and by actual energy comparison (in order to determine the first-order phase transformations).

The phase diagram is shown in Fig. 15. Keeping in mind the correspondence between the transition metals and the parameters $n$ and $C_0/E''$, one sees that the phase diagram is in reasonable semiquantitative agreement with the observed incidence of magnetism in transition metals and their alloys in that ferromagnetism occurs in the upper right-hand portion of the phase diagram and complex magnetic states occur towards the center of the band. Ferromagnetism is seen to be possible when $C_0/E''>3.5$. If it is assumed that the effect of the five $d$ bands is simply to increase the density of states by a factor of 5 over that found in our one band model, and if we further assume a bandwidth of about 4.5 eV, then one finds $C_0\sim\frac{1}{2}$ eV which may be compared to the values of roughly 1 eV in Ni[20] and 0.7 eV in Fe.[21]

The possibility of a nonparamagnetic ground state for very small values of $C_0/E''$ as occurs in the center of the band is directly related to the coincidence of the Fermi surface and the magnetic zone boundary. In the case of a more realistic band structure where this coincidence cannot occur, one would expect to find only the paramagnetic state for small $C_0/E''$ as is observed in the $4d$ and $5d$ transition series. As $C_0/E''$ is increased above some critical value, the antiferromagnetic state would be attainable for some restricted range of valence and as $C_0/E''$ is further increased, the ferrimagnetic state might become stable. The special ferrimagnetic state occupies a large region in phase space compared to the antiferromagnetic state while, in fact, antiferromagnetism is usually observed to occur; this failure of the model may be due to the one band approximation which does not take account of intra-atomic exchange or to the rather simplified treatment of electron correlation.

We note that the phase transformation of the paramagnetic state to the antiferromagnetic or ferromagnetic states is second order. This result leads one to believe that the actual region of stability of the paramagnetic state has, in fact, been determined from the calculation of the paramagnetic susceptibility $\chi(\mathbf{q})$ for general $\mathbf{q}$. All phase transformations that do not involve the paramagnetic state (with the exception of the ferromagnetic to SSDW transformation) are first order; thus, the response function method has been useful for determining the boundary lines denoting phase transformations only in those special cases.

The question of whether or not a local magnetic moment can be formed at an impurity site of a transition metal has been investigated and the results are summarized in Fig. 16. For a given $n/N$ there is a minimum value of $C_0/E''$ (indicated by the lower dashed line of the figure) below which no moment formation is possible and above which moment formation is possible depending on the value of $V_I$. For sufficiently large $C_0/E''$ (indicated by the upper dashed line of the figure) local moment formation takes place in the case $V_I=0$ indicating an instability in the host metal. It is to be emphasized that any condition for local moment formation that is independent of $V_I$ must, in fact, refer to an instability of the host metal itself.

Beck *et al.*[21] have measured the linear specific heat $\gamma T$ of a number of bcc $3d$ alloys, and they found a sharp peak in $\gamma$ in several alloy systems when the electron to atom ratio is about 6.5. We suggest that part of the peak is due to the presence of a magnetic zone structure at least in the case of $Cr_{0.5}Mn_{0.5}$ which exhibits the largest

[20] J. C. Phillips, Phys. Rev. **133**, A1020 (1964).
[21] C. H. Cheng, C. T. Wei, and P. A. Beck, Phys. Rev. **120**, 426 (1960).

peak. Such a peak is exemplified in our model; in the case of the $q=\pi/a(1,1,1)$ antiferromagnetic state the density of states is porportional to $\eta_0(\epsilon)(\epsilon^2+A_Q^2)^{1/2}/\epsilon$ which peaks as $\epsilon \to 0$.

## ACKNOWLEDGMENTS

The author is indebted to Dr. M. H. Cohen for having suggested the problem and for maintaining a flow of very helpful and stimulating correspondence during his sabbatical. It is a pleasure to thank Dr. L. M. Falicov for a number of very profitable discussions.

I am grateful to the National Science Foundation and the U. S. Office of Naval Research for direct financial support of this work. In addition, the research benefited from partial support of related solid-state theory by NASA and general support of the Institute for the Study of Metals by ARPA and the NSF.

## APPENDIX A

In order to derive Eq. (5.5) we introduce the resolvents $R$ and $R_0$ defined by

$$R(z)=(z+\mu-H)^{-1}, \tag{A1}$$

$$R_0(z)=(z+\mu_0-H_0)^{-1}, \tag{A2}$$

where $\mu$ and $H$ are the Fermi energy and SCF Hamiltonian in the presence of an external magnetic field and $\mu_0$ and $H_0$ refer to the case of no magnetic field. The relation

$$R=R_0+R_0(H_1-\mu_1)R, \tag{A3}$$

where $H_1=H-H_0$ and $\mu_1=\mu-\mu_0$ leads to the first-order approximation

$$R=R_0+R_0(H_1-\mu_1)R_0. \tag{A4}$$

The density matrix $\rho=\rho_0+\rho_1$ can be expressed as

$$\rho=(1/2\pi i)\oint dz\, R(z)(e^{\beta z}+1)^{-1}, \tag{A5}$$

where the contour of integration includes all the eigenvalues of $H$. Equations (A4) and (A5) yield

$$\rho_1=(1/2\pi i)\oint dz\, R_0(H_1-\mu_1)R_0(e^{\beta z}+1)^{-1}. \tag{A6}$$

Upon taking the matrix element of $\rho_1$ with respect to eigenfunctions of $H_0$ and carrying out the complex integration we obtain Eq. (5.5).

In order to illustrate the procedure used in calculating a response function we shall evaluate the ferromagnetic susceptibility $\chi_z(\mathbf{q})$. Equation (5.2) yields

$$\langle l\uparrow|V_R|l\uparrow\rangle=\sum_{\mathbf{k}\sigma\mathbf{k}'\sigma'}\langle\mathbf{k}\sigma|\rho_1|\mathbf{k}'\sigma'\rangle\langle\mathbf{k}'\sigma',l\uparrow|O|l\uparrow,\mathbf{k}\sigma\rangle, \tag{A7}$$

where $|\mathbf{k}\sigma\rangle$ denotes a spin-$\sigma$ eigenfunction of the unperturbed ferromagnetic state and $|l\sigma\rangle$ denotes a Wannier function of spin $\sigma$. The relation $\langle\mathbf{k}'\sigma'|=\sum_{l'}\langle\mathbf{k}'\sigma'|l\sigma'\rangle\langle l\sigma'|$ in conjunction with Eqs. (2.5), (5.3), and (A7) gives

$$\langle l\uparrow|V_R|l\uparrow\rangle=(C_0/N)\sum_{\mathbf{k}\mathbf{k}'}\langle\mathbf{k}\uparrow|\rho_1|\mathbf{k}'\downarrow\rangle \times\exp[i(\mathbf{k}'-\mathbf{k})\cdot\mathbf{R}_l], \tag{A8}$$

hence

$$V_{R\uparrow}(\mathbf{q})=(C_0/N)\textstyle\sum_{\mathbf{k}}\langle\mathbf{k}\downarrow|\rho_1|\mathbf{k}+\mathbf{q}\downarrow\rangle, \tag{A9a}$$

similarly,

$$V_{R\downarrow}(\mathbf{q})=(C_0/N)\textstyle\sum_{\mathbf{k}}\langle\mathbf{k}\uparrow|\rho_1|\mathbf{k}+\mathbf{q}\uparrow\rangle. \tag{A9b}$$

From (5.5) and $H_{1\sigma}(\mathbf{q})=\langle\mathbf{k}\sigma|H_1|\mathbf{k}+\mathbf{q}\sigma\rangle$, we obtain

$$V_{R\uparrow}(\mathbf{q})=\Gamma_\downarrow(\mathbf{q})(H_{1\downarrow}(\mathbf{q})-\delta_{\mathbf{q},0}\mu_1), \tag{A10a}$$

$$V_{R\uparrow}(\mathbf{q})=\Gamma_\uparrow(\mathbf{q})(H_{1\uparrow}(\mathbf{q})-\delta_{\mathbf{q},0}\mu_1), \tag{A10b}$$

where

$$\Gamma_\sigma(\mathbf{q})=(1/N)\textstyle\sum_{\mathbf{k}}(F_{\mathbf{k}+\mathbf{q}\sigma}-F_{\mathbf{k}\sigma})/(\epsilon_{\mathbf{k}+\mathbf{q}\sigma}-\epsilon_{\mathbf{k}\sigma}). \tag{A11}$$

Equation (5.6) yields

$$\mu_1=\left(\sum_{\mathbf{k}\sigma}\langle\mathbf{k}\sigma|H_1|\mathbf{k}\sigma\rangle\left(\frac{\partial F}{\partial\epsilon}\right)_{\mathbf{k}\sigma}\right)\Big/\left(\sum_{\mathbf{k}\sigma}\left(\frac{\partial F}{\partial\epsilon}\right)_{\mathbf{k}\sigma}\right), \tag{A12}$$

which can be rewritten as

$$\mu_1=(H_{1\downarrow}(0)\Gamma_\downarrow(0)+H_{1\uparrow}(0)\Gamma_\uparrow(0))/(\Gamma_\downarrow(0)+\Gamma_\uparrow(0)), \tag{A13}$$

where

$$\Gamma(0)=\lim_{\mathbf{q}\to 0}\Gamma(\mathbf{q}). \tag{A14}$$

The quantity $-\Gamma_\sigma(0)$ is just the density of states of the spin-$\sigma$ band at the Fermi surface. Recalling that $H_1(\mathbf{q})=V_R(\mathbf{q})+H'(\mathbf{q})$ where $H'(q)=-\mu_B\boldsymbol{\sigma}\cdot\mathbf{B}(\mathbf{q})$ and making use of Eqs. (5.8a) and (A10) we obtain

$$\chi_z(\mathbf{q})=\mu_B{}^2(-\Gamma_\downarrow(\mathbf{q})-\Gamma_\uparrow(\mathbf{q})+2C_0\Gamma_\uparrow(\mathbf{q})\Gamma_\downarrow(\mathbf{q}))/(1-C_0{}^2\Gamma_\downarrow(\mathbf{q})\Gamma_\uparrow(\mathbf{q})) \tag{A15}$$

for $\mathbf{q}>0$. In the case of $\mathbf{q}=0$ we find

$$\chi_z(0)=-4\mu_B{}^2/[2C_0+(1/\Gamma_\uparrow(0))+(1/\Gamma_\downarrow(0))]. \tag{A16}$$